A KINETIC INVESTIGATION OF 1,3-DIPOLAR CYCLOADDITIONS OF AZIDOPYRIDINE-*N*-OXIDES

A THESIS

SUBMITTED TO THE GRADUATE SCHOOL

IN PARTIAL FULFILLMENT OF THE REQUIREMENTS

FOR THE DEGREE OF

MASTER OF SCIENCE

BY

BREANNA M. RICKETTS

ADVISOR: DR. JAMES S. POOLE

BALL STATE UNIVERSITY

MUNCIE, INDIANA

MAY 2015

A KINETIC INVESTIGATION OF 1,3-DIPOLAR CYCLOADDITIONS

OF AZIDOPYRIDINE-N-OXIDES

A THESIS

SUBMITTED TO THE GRADUATE SCHOOL

IN PARTIAL FULFILLMENT OF THE REQUIREMENTS

FOR THE DEGREE

MASTER OF SCIENCE

BY

BREANNA M. RICKETTS

Committee Approval:

Committee Chairperson	Date
Committee Member	Date
Committee Member	Date

Departmental Approval:

Departmental Chairperson	Date
Dean of Graduate School	Date

BALL STATE UNIVERSITY
MUNCIE, INDIANA
May 2015

Acknowledgements

I would like to convey my gratitude to:

Dr. Poole for being an excellent mentor, motivator, and believer throughout the course of my project. My committee members, Dr. Lang and Dr. Tye for preparing me for the future. The Ball State Department of Chemistry faculty and staff to help out whenever it was needed.

My husband Andrew: you have been with me through the good times and the bad. You have donated your time and artistic talent which has made my thesis become a reality. Another huge thank you for having the ability to make me smile and laugh even when I really didn't want to do so.

My Mom and Granny: Mom, thanks for constantly believing in me and being my number one fan. Thank you for the many hours of phone calls at all hours of the day.
Granny, thank you for being the best grandma in the world. You opened your home and supported me through some of my rough times and for that "I just love you to pieces."

Mom and Dad Robinson: Thank you for being the best in-laws a wife could ever ask for. Mom, thank you for all of the meals you prepared so that I had a chance to work on my thesis. Your kindness, forethought, and encouragement helped me succeed. Dad, thank you for supporting me when you had the chance. I take some happiness knowing that you would have been proud of me had you been here to witness my achievement.

ABSTRACT

THESIS: The Kinetics of 1,3-Dipolar Cycloadditions of Azidopyridine *N*-Oxides

STUDENT: Breanna Ricketts

DEGREE: Master of Science

COLLEGE: Sciences and Humanities

DATE: May 2015

PAGES: 48

1,3-dipolar cycloaddition reactions of aromatic azides and alkenes or alkynes to form triazole and triazolines is a well established reaction. Reaction rate studies for phenyl azide with a variety of dipolarophiles have been previously performed by Huisgen, and then the reactivity and selectivity of those reactions were later explained by Sustmann in FMO terms. However, Sustmann did not use the entire set of reaction rates, since not all the FMO data were known at the time.

The first half of this thesis employed the use of computational chemistry to determine Frontier Molecular Orbital energies of the to determine the complete set of Huisgen and to generate a complete and updated FMO correlation diagram for phenyl azide cycloadditions, to determine the applicability of the Sustmann model for a broader range of dipolarophiles. The second half of this thesis was to experimentally determine the reaction rates of 1,3-dipolar cycloaddition reactions with azidopyridine *N*-oxides and a wide range of dipolarophiles in order to determine the role that the *N*-oxide group plays with respect to the reactivity and selectivity in 1,3-dipolar cycloaddition reactions of the azide moiety. In addition, these azidopyridine 1-oxides were observed to undergo tandem cycloaddition that is not seen with phenyl azide.

Table of Contents

List of Tables

List of Schemes

List of Figures

Chapter 1 - Literature Background

1.1 Introduction – A Brief Overview of the Chemistry of Aryl Azides

The chemistry of alkyl and aryl azides has been extensively studied over the years in large part due to their utility in synthetic organic chemistry, materials science, and biochemistry. Alkyl and aryl azides exhibit a diverse range of reactivity, which is broadly summarized in Scheme 1.

Scheme 1: Major Modes of Reactivity for Alkyl and Aryl Azides

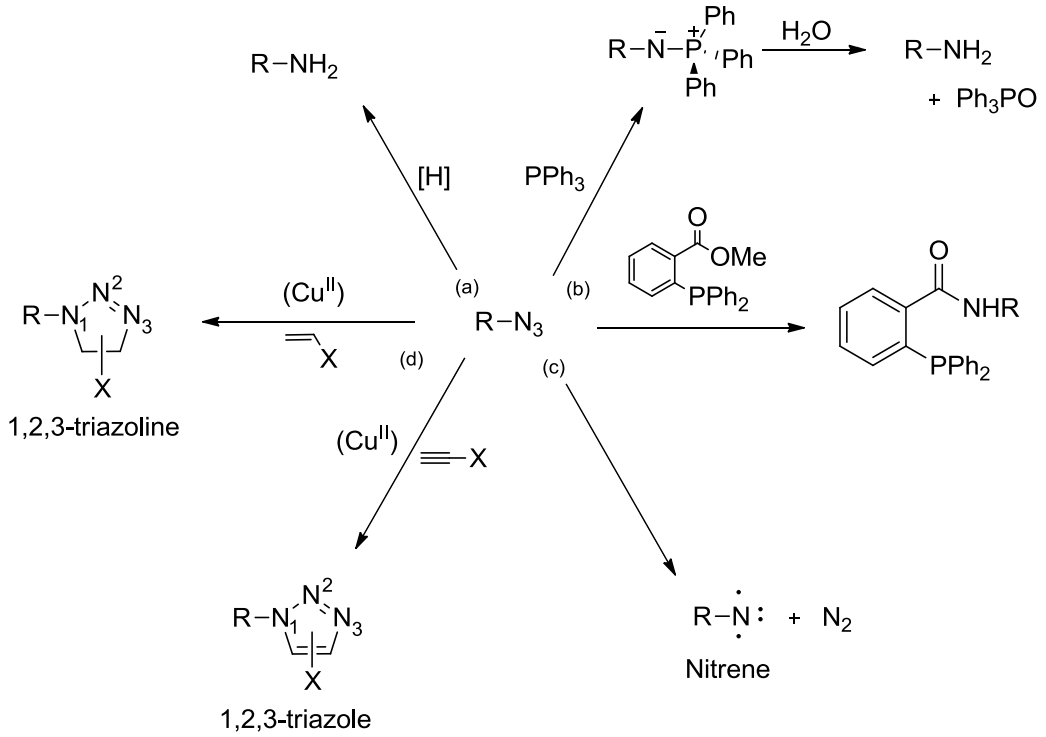

The reactivity of azides may be described in terms of four broad groups:

(a) *Reduction to amines*: this may be achieved by well known hydride reducing agents such as $LiAlH_4$.[1]

(b) *Formation of aza-ylides by reaction with phosphines* (the Staudinger reaction). Once formed, these aza-ylides react with water to yield amines.[2] However, modification of the aryl ring on the phosphine group (*o*-substitution with an ester for example) results in the formation of an amide in aqueous solution, a reaction known as the Staudinger ligation.[3]

(c) *Thermal or photochemical generation of nitrenes*. Nitrenes are highly reactive species that have only six valence electrons. Aromatic azides may be employed as photoresists, compounds that generate chemically resistant polymeric materials on exposure to light. Such materials are used in the processes of photolithography, or photoengraving to form a patterned coating on a surface.[4] Other uses of nitrene chemistry include bioaffinity labeling, where a photochemically derived nitrene inserts into biomolecules as tags or labels.[5] Photochemistry involving aryl nitrenes produces synthetically useful azepine and carbazole derivatives.[6,7]

(d) *1,3-Dipolar cycloadditions*.[8] 1,3-dipolar cycloadditions of azides are used to synthesize 1,2,3-triazole and triazoline rings. These reactions are often efficiently catalyzed with copper salts (so-called "click" reactions),[9] and have found widespread use, particularly with alkynes in bioconjugation reactions.[10] The aromaticity and UV-visible properties of the formed triazoles (appropriately

substituted with chromophoric groups) have made "click" chemistry useful for bioimaging purposes.[11] .

A group of particularly interesting aryl azides are the azidopyridine and quinoline-*N*-oxides, such as 2-, 3-, and 4-azidopyridine *N*-oxide (**1**-**3** respectively) and 4-azidoquinoline *N*-oxide (**4**). (Scheme 2).

Scheme 2: Some Representative Azidoheteroarene *N*-Oxides

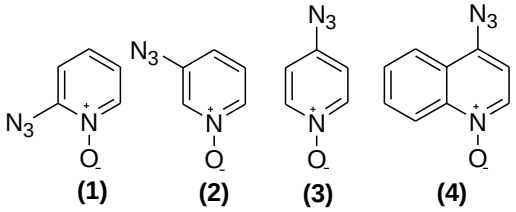

The *N*-oxide group is a potentially useful group, as it is known to enhance the water solubility of aromatic compounds, making it a potentially useful substrate for aqueous (biological) applications. In addition, the *N*-oxide group has an electronic structure that makes it capable of acting as both an electron-donating and an electron-withdrawing group. (Scheme 3).

Scheme 3: *N*-oxide Group as a Potential Electron-Donating and Electron-Withdrawing Group

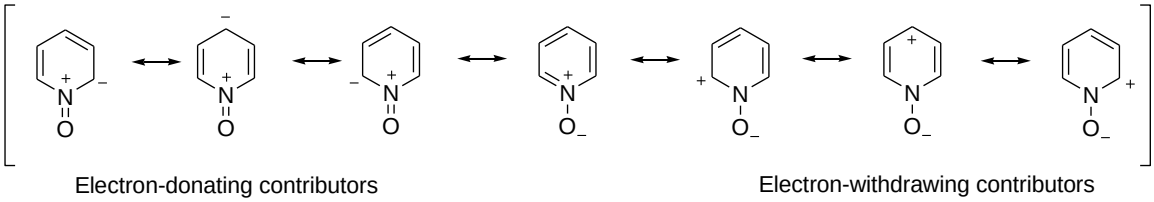

The presence of the *N*-oxide group has the potential to alter the electronic structure of the aryl ring, which in turn may affect the reactivity of these species relative to the parent

phenyl azide. The nitrene chemistry of the species in Scheme 2 have been previously investigated,[12-14] and it has been demonstrated that the nature and position of the *N*-oxide moiety on the ring has profound effects on nitrene chemistry. Comparatively, little is known about the 1,3-dipolar cycloaddition chemistry of these species. This study addresses the kinetics, regioselectivity and structure-reactivity relationships of the 1,3-dipolar cycloadditions of **2** and **3**.

1.2 1,3-Dipolar Cycloaddition Reactions of Aryl Azides

1.2.1 General Features of the 1,3-Dipolar Cycloaddition Reaction

The term 1,3-dipolar cycloaddition refers to a group of reactions that are widely used in synthetic organic chemistry to generate five-membered heterocyclic systems that are not readily accessible by other means. A diverse group of reagents may undergo such reactions to yield different products, but all reactions share certain features in common (Scheme 4). Reaction occurs between two species that are typically identified as a 1,3-dipole (represented as $a=b^{+}\text{-}c^{-}$ in the generalized reaction) and an unsaturated system, known as a dipolarophile (represented by d=e). Dipolarophiles are typically alkenes or alkynes, and a wide range of possible 1,3-dipoles are available to synthetic chemists. All 1,3-dipoles have an allylic π-system, whereby four electrons are distributed in three overlapping atomic p-orbitals, and the system is stabilized by resonance. Since the 1,3-dipole is typically neutral overall, atoms within the moiety carry formal charges. The onium center, b, compensates for the negative charge that is shared between ends a and c. Certain 1,3-dipoles, like azide, have an additional π-bond in a perpendicular plane to the

allyl anion molecular orbital (MO). The presence of this extra π-bond makes the 1,3-dipole linear, rather than bent.[8]

Scheme 4: Generalized 1,3-Dipolar Cycloaddition

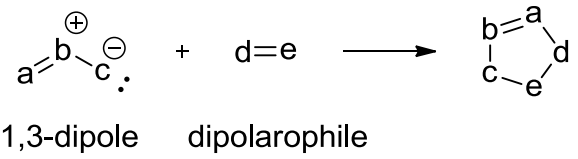

One may consider the reaction of phenyl azide with a dipolarophile to be representative of aryl azides, and to some extent, of dipolarophiles in general (Scheme 5).

Scheme 5: Potential Reactions of Phenyl Azide with Substituted Alkenes

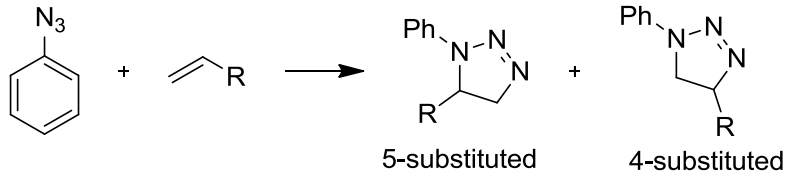

The reaction between phenyl azide and an alkene generates a 1,2,3-triazoline ring. The reaction between phenyl azide and *E*/*Z*- diastereomers of olefins is stereospecific, in that substituents on the same side of the double bond will end up on the same face of the formed triazoline ring. Observed regioselectivity is dependent upon the substitution on the alkene by electron-donating or electron-withdrawing groups. This suggests that the mechanism is concerted, and the dipole/dipolarophile system constitutes a [4π + 2π] reaction that is thermally allowed under the Woodward-Hoffmann rules for pericyclic reactions.[15] The transition state geometry positions the dipolarophile in a plane with the azide occupying a separate parallel plane either above or below to maximize the degree

of π-orbital overlap which will lead to eventual σ-bond formation (Figure 1).[8] High-level theoretical calculations for these reactions generally support this picture of a concerted transition state, although not necessarily the synchronous bond formation shown in Figure 1.[16,17]

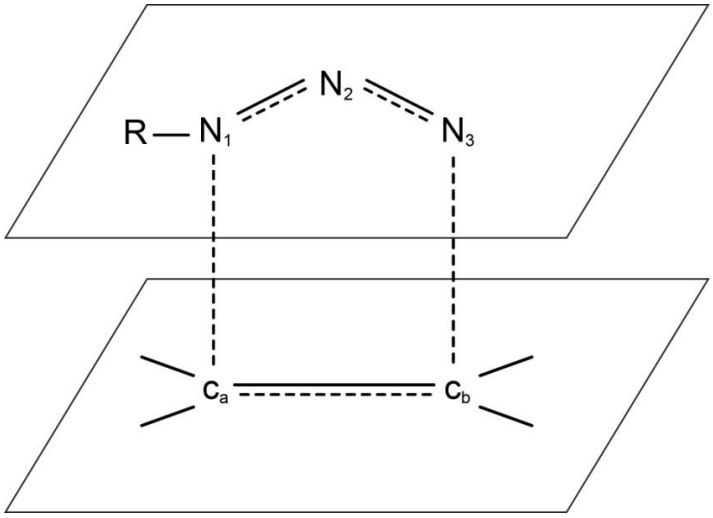

Figure 1. Qualitative representation of the transition state for an azide reacting with a dipolarophile. Note that the azide lies in a plane parallel to the dipolarophile plane.

Scheme 5 shows that there are two possible regiochemical outcomes for monosubstituted alkenes. Previous experiments have determined that electron-withdrawing groups on the alkene favor the formation of the 4-substituted product with high degrees of regioselectivity.[18] On the other hand, an electron donating group favors the formation of the 5-substituted product. In cases where there is a lack of strong electronic substituents a mixture of products is observed.[18] Any model for these reactions must be capable of predicting these regiochemical outcomes.

1.2.2 Frontier Molecular Orbital Description of 1,3-Dipolar Cycloadditions

The concerted nature of the cycloaddition reaction suggests that the rate and outcome of reactions are subject to molecular orbital control, both in terms of the symmetry and energies of the interacting π-molecular orbitals. One may define an interaction energy ΔE for the interaction of occupied and unoccupied orbitals in the azide (A) – olefin (O) reacting pair:

$$\Delta E = 2\sum_{O}^{occ}\sum_{A}^{unoc}\frac{\sum_{i,j}\left(c_{Oi}c_{A,j}\beta_{ij}\right)^2}{(E_O - E_A)} + 2\sum_{O}^{unoc}\sum_{A}^{occ}\frac{\sum_{i,j}\left(c_{Oi}c_{A,j}\beta_{ij}\right)^2}{(E_O - E_A)} \qquad (1)$$

where E_O and E_A are the energies of molecular orbitals O and A on the olefin and azide respectively. The coefficients $c_{O,i}$ correspond to the contribution of the atomic orbital *i* to the linear combination of atomic orbitals (LCAO) that describes molecular orbital O, and coefficients $c_{A,j}$ are similarly defined. Finally, β_{ij} is the resonance integral for orbitals I and j, which describes the degree of stabilization that occurs when electrons are shared between the atomic orbitals (*ie*. the beginnings of the formation of a covalent bond).

It is probably useful to note that equation (1) corresponds to a single term in a more complex expression known as the Salem-Klopman equation, which is based on a perturbation treatment of the reacting system.[19-22] We make the assumption that for olefins reacting with a single azide, the remaining terms (which describe the repulsion of the interacting electron densities, and any Coulombic terms) are constant, and differential reactivity arises from differences in orbital interactions described in equation (1). It is also important to note that a perturbation treatment requires small changes in the energy and structures of the reactants, meaning that this approach is most effective in describing exothermic reactions. Frontier Molecular Orbital (FMO) Theory proposes that the

dominant MO interactions that define the reactivity and selectivity of reaction are those between the highest occupied molecular orbital (HOMO) of one reactant and the lowest unoccupied molecular orbital (LUMO) of the other reactant.[23] Taking this into account, and making the further approximation that $c_{Oi}c_{Aj}\beta_{ij}$ are similar in magnitude over a range of olefin substrates, equation (1) reduces to the simple form:

$$\Delta E = K\left[\frac{1}{E_{OHo} - E_{ALu}} + \frac{1}{E_{AHo} - E_{OLu}}\right] \qquad (2)$$

where K becomes a parameter that characterizes the overlap of between the molecular orbitals of the reactant pair, E_{OHo} and E_{OLu} are the HOMO and LUMO energies of the olefin respectively, and E_{AHo} and E_{ALu} are the HOMO and LUMO energies of the azide respectively. ΔE is a stabilizing term, that lowers the activation barrier to reaction. It is clear from Equation (2), that the FMO interactions that dictate the reactivity and selectivity of reaction are those where the difference in the HOMO-LUMO energies is smallest.

Figure 2 shows the frontier molecular orbitals and their energies for a reacting pair of phenyl azide and styrene, and indicates that the reaction is controlled by the interactions of the HOMO of styrene and LUMO of phenyl azide. It is worth noting that the nature of the HOMO-LUMO interaction also has regiochemical consequences (see below).

The MO treatment of a pericyclic reaction such as a 1,3-dipolar cycloaddition requires the symmetry of the molecular orbitals correlate, meaning that the p-orbitals used in the LCAO description of the MO that are situated on the pairs of reacting atoms (a and d, c and e in the generalized reaction in Scheme 4) are in phase. In phase means

that the bonding and antibonding lobes of both species matches with each other creating a constructive orbital interaction that ultimately leads to bond formation between those atoms. In cases where the molecular orbitals are not in phase, such as photochemical reactions, then there is an absence of this constructive orbital overlap and no new bond formation occurs.

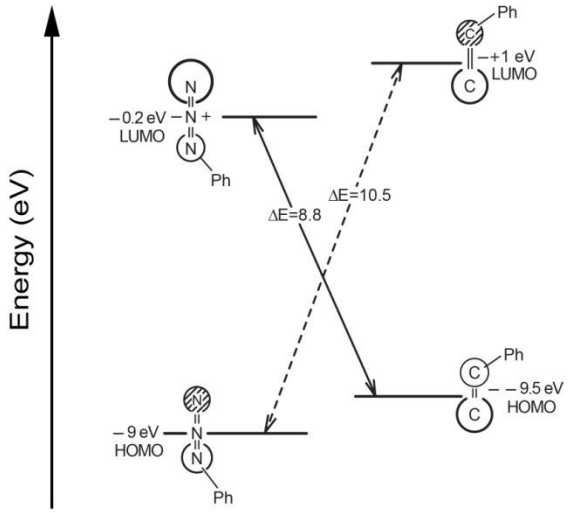

Figure 2: HOMO and LUMO correlations for 1,3-dipolar cycloaddition between phenyl azide and styrene

One may consider a range of dipolarophiles, substituted with electron-donating groups, electron-withdrawing groups, and groups that do not exhibit significant electronic effects. Electron-donating groups on the dipolarophile will raise both its HOMO and LUMO energies, whereas an electron-withdrawing group will lower both the HOMO and LUMO energies. The changes in the HOMO and LUMO energies that arise from the substituents is considerably smaller than the HOMO-LUMO gap of the dipolarophile. By observing the structure-reactivity behavior of 1,3-dipoles with a range of substituted olefins, one may discern three basic types of 1,3-dipole, shown qualitatively in Figure 3:

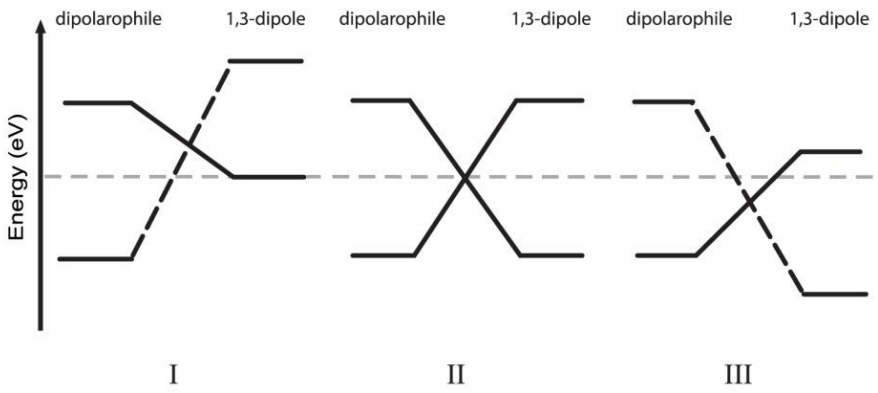

Figure 3: Energy level diagrams for the FMOs of dipoles and dipolarophiles engaged in a 1,3-dipolar cycloaddition reaction. Major or dominant interactions are shown by solid lines, minor interactions by dashed lines.

- A Type I 1,3-dipole is characterized by a relatively high energy HOMO, which means for all dipolarophiles, the HOMO(dipole)-LUMO(dipolarophile) interaction is dominant. Dipoles of this type, which include diazoalkanes and nitrile ylides, are considered nucleophilic.
- A Type III dipole is characterized by a low-lying LUMO, which means that for all dipolarophiles, the HOMO(dipolarophile)-LUMO(dipole) interaction is dominant. These electrophilic dipoles include species such as ozone.
- A Type II 1,3-dipole, such as an azide or a nitrile oxide, has HOMO and LUMO energies that are similar to that of the dipolarophiles. Under these circumstances, small differences due to substituents on the dipolarophile can have an effect on which of the interactions is dominant.

Each type of dipole will exhibit a characteristic functional form in a plot of the interaction energy as a function of substituent electron-donation and withdrawal (which

reflects the HOMO energy). Type I 1,3-dipoles (nucleophiles) will have greater interaction energies with olefins substituted with electron withdrawing groups, Type III 1,3-dipoles will show the opposite behavior. Type II 1,3-dipole behavior will appear as a superposition of both Type I and Type III. Interaction energy is a stabilizing influence that lowers the energy of the transition state and thus enhances the rate of reaction. As with many structure-reactivity studies, it is assumed that the entropic components (the Arrhenius pre-exponential) remain effectively unchanged over a range of similar substrates.

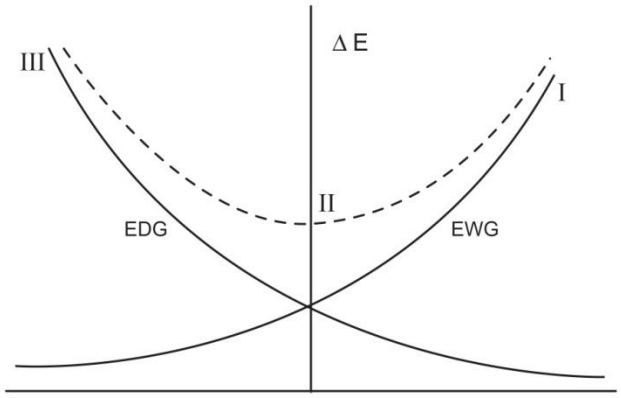

Figure 4. The effect of substitution on the dipolarophile on the interaction energy ΔE (Eq.1) of reacting 1,3-dipole/dipolarophile pairs.

For a dipolarophile with multiple substituents, one may envisage cases where the both types of substituent are present, electron-withdrawing and electron-donating. In such cases, the counteracting substituents will lead to no, or very small rate enhancements relative to an unsubstituted dipolarophile. On the other hand, if there is more than one substituent of the same type on the dipolarophile, then a synergistic effect is observed.[24]

1.2.3 Substituent Effects and Regioselectivity

Scheme 5 above indicates that 1,3-dipolar cycloaddition of azides to olefins (or alkynes) can lead to the formation of two regioisomers, where electron withdrawing groups favor the formation of the 4-regioisomer, and electron donating groups favor the 5-regioisomer. In order to explain this regioselectivity, we must not only consider the energies of the orbitals, but also their topology.

Figure 5 illustrates the orbital interactions for phenyl azide reacting with a dipolarophile with an electron withdrawing group ($HOMO_{azide}$-$LUMO_{olefin}$ dominant) and an electron-donating group ($HOMO_{olefin}$-$LUMO_{azide}$ dominant). All MOs are distorted from their nominal allyl/olefin π-MOs due to the asymmetry of each reactant – the size of the p-orbital lobes in Figure 5 qualitatively reflect the orbital coefficients, $c_{i,A/O}$ for the p-orbitals in the LCAO descriptions of the MOs (see Equation 1, above). Molecular arrangements where both orbital coefficients of the interacting p-orbitals (or the p-orbital components of the MOs) are large are more favorable than those where only one or none of the coefficients are large (illustrated by the $c_{O,i}c_{A,j}\beta_{ij}$ terms in equation 1).

The more favored arrangements for dipolarophiles with electron withdrawing and electron donating substituents are shown in Figure 5, and these are consistent with the observed regioselectivity. The transition states for the favored arrangements are lower in energy (and typically earlier) than those for other arrangements.

In each of these cases, the asymmetry of the MOs imply that the orbitals with larger coefficients will interact to a greater extent than those without – one of the bonds will be in greater evidence ("more formed") in the transition state than the other. Such reactions are often described as concerted (all bonds formed in a single mechanistic step

with no observable intermediates), and asynchronous (bonds are not formed to the same extent at any given point along the reaction coordinate). High-level MO calculations confirm the asynchronous nature of these reactions.[16] Typically, a high degree of symmetry in the reacting system is required for a reaction to be synchronous.

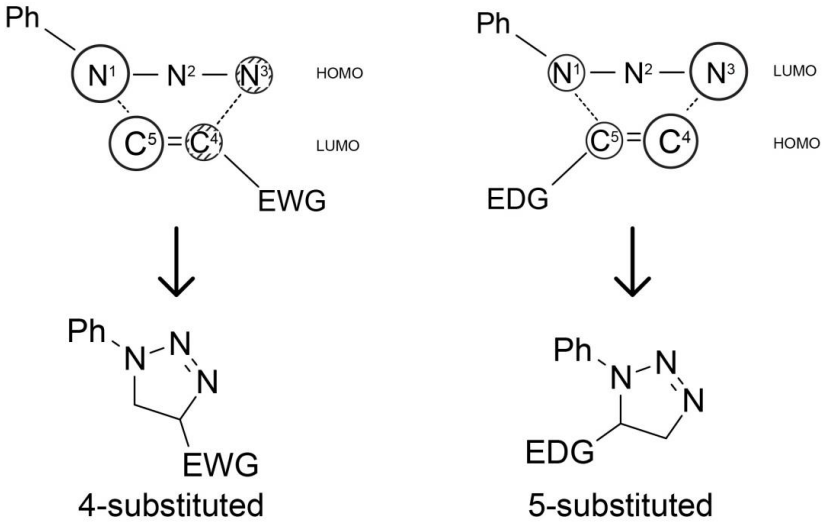

Figure 5. MO interactions of phenyl azide and substituted olefins responsible for experimentally observed regioselectivity. The size of the circles reflect orbital coefficients in the LCAO. For reasons of clarity, the coefficients at N^2 are not shown.

1.3 Experimental Studies of the Cycloaddition Reactions of Phenyl Azide

In order to construct structure-reactivity correlations for the reaction of phenyl azide with substituted olefins, one must have a quantitative measure of the substituent effect. The empirical "substituent parameter", such as those formulated by Hammett and others is one useful approach,[25,26] but for correlations based on Equations 1 and 2 above, it may be more useful to have an experimental measure of the HOMO and LUMO energies of the reagents.

The energy of the HOMO can be experimentally determined by measurement of the ionization potential of a molecule - the smallest amount of energy required to remove an electron from the outermost sub-shell, which in principle should involve removal of an electron from the HOMO. Koopmans' theorem[27] postulates that to good approximation the first ionization potential of a molecule is equivalent in magnitude (but opposite in sign) to the energy of the HOMO.

The LUMO energy can be experimentally determined by measurement of the electron affinity of a molecule - a measure of the capacity of an atom to accept an extra electron into the outermost sub-shell. Koopmans' theorem postulates that the extra electron will populate the LUMO, and that to good approximation the electron affinity will have equal magnitude and opposite sign to the energy of the LUMO.[27] One should note that it is not always possible to measure both the ionization potential, and the electron affinity of molecules experimentally.

The first studies of the kinetics of phenyl azide 1,3-dipolar cycloadditions was performed by Huisgen *et al*., who measured the rate coefficients for reaction of phenyl azide and 30 variously substituted olefins under pseudo first order conditions at 25°C (Table 1)[28]. The correlation between the reaction rate coefficients and orbital energies for these reactions was reported by Sustmann[24,29] who plotted the rate coefficients for each olefin as a function of their corresponding ionization potentials (Figure 6). The resulting correlation curve has the positive curvature that is consistent with Type II dipole behavior described by FMO theory.

Table 1. Rate coefficients for reaction of phenyl azide with dipolarophiles (Huisgen)

	$\log_{10}(k_{cyc}.M^{-1}s)$		$\log_{10}(k_{cyc}.M^{-1}s)$
Electron-donating groups		*Electron-withdrawing groups*	
n-butyl vinyl ether	-7.40	ethyl acrylate	-6.01
1-ethoxycyclopentene	-7.31	acrylonitrile	-6.97
1-pyrrolidinocyclopentene	-1.94	dimethyl maleate	-7.47
1-pyrrolidinocyclohexene	-3.00	methyl methacrylate	-7.14
N-(1-cyclopentenyl)morpholine	-3.59	diethyl fumarate	-6.08
styrene	-7.40	maleic anhydride	-6.14
4-methoxystyrene	-7.25	ethyl crotonate	-7.57
4-methylstyrene	-7.29	ethyl cinnamate	-8.02
4-chlorostyrene	-7.40	*N*-phenylmaleimide	-5.56
Hydrocarbons		*Alkynes*	
cyclopentene	-6.73	phenylacetylene	-7.54
cyclohexene	-8.48	methyl propiolate	-5.98
bicyclo[2.2.1]hept-2-ene	-4.73	ethyl phenylpropiolate	-7.68
bicyclo[2.2.1]hepta-2,5-diene	-4.71	dimethyl acetylenedicarboxylate	-5.60
bicyclo[2.2.2]oct-2-ene	-7.05		
hept-1-ene	-7.62		
1-methylcyclopentene	-7.62		
isoprene	-7.82		

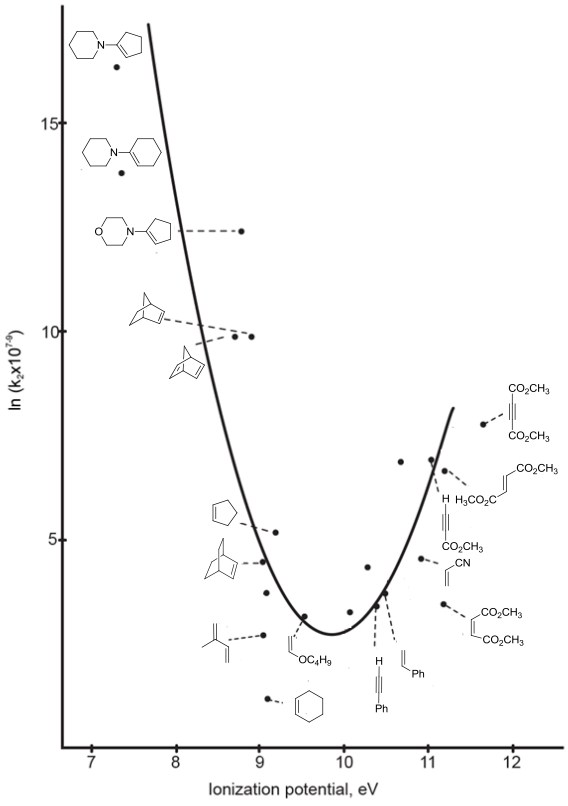

Figure 6. Sustmann correlation of rate coefficients for the reaction of various olefins with phenyl azide with their corresponding ionization potentials (HOMO energies).

Examining the Sustmann correlation (Figure 6), the electron-donating groups on olefins are located on the left and the electron-withdrawing groups on olefins are located on the right. Groups with no strong electronic groups are seen at the base of the fitted parabolic line. It should be noted that electron donation/withdrawal effects are reversed from those shown in Figure 4.

1.4 Tandem Cycloaddition Reactions

The reaction of compounds **2** and **3** with methyl acrylate in acetonitrile lead to the formation of compounds **5** and **6**[30] respectively.

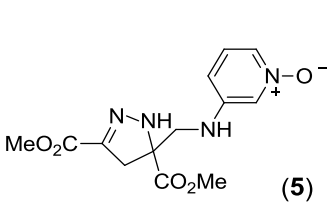

(**5**)

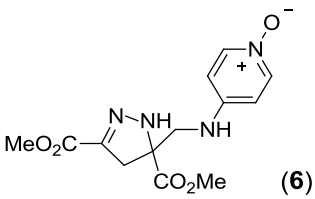

(**6**)

Similar reactions have been observed for simple aryl azides, but typically occur at long reaction times, with low yields and low regioselectivity.[31] Yadav *et al*.[31] have demonstrated that simple aryl azides will undergo such reactions with the addition of a strong organic base such as DABCO (Bayliss-Hillmann conditions), but limited their study to electron deficient olefins such as the acrylate esters. Their proposed mechanism (Scheme 6) involves the deprotonation of the 1,2,3-triazoline to generate an enolate anion, that subsequently fragments. Reprotonation of the rearranged species generates a diazoalkane intermediate, which itself can act as a 1,3-dipole (In principle, a Type I dipole, see above), and reacts with a second equivalent of dienophile to generate the pyrazoline products.

Scheme 6: Mechanism of Pyrazoline Formation From Phenyl Azide and Methyl Acrylate

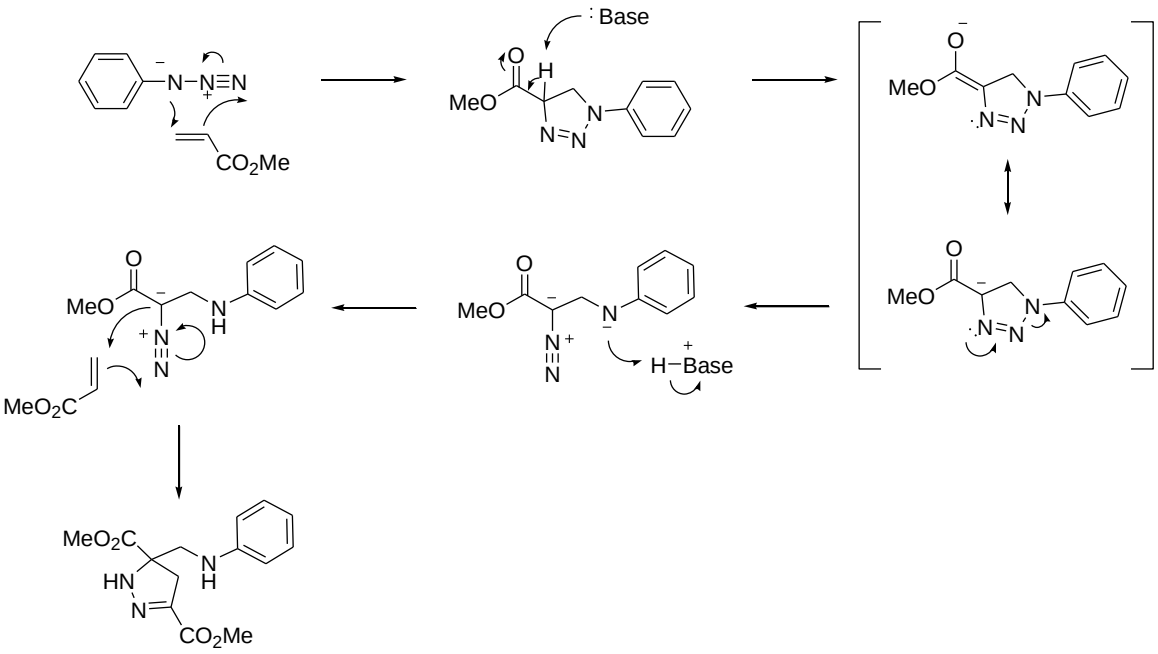

In the case of the azidopyridine *N*-oxides, the presence of an organic base is not required, and it was found that the addition of bases such as DABCO or triethylamine made no discernible difference to the rate of reaction.[30] This suggests that the first 1,3-dipolar cycloaddition is the rate limiting step, and that the presence of the *N*-oxide group greatly enhances the acidity of the first cycloadduct.

This contribution describes a combined kinetic and computational study to characterize the structure-reactivity relationships in the 1,3-dipolar cycloaddition chemistry of azidopyridine *N*-oxides in terms of FMO theory, in order to understand how the presence of the *N*-oxide moiety affects the electronic structure of the aryl ring, and what synthetic consequences arise from such a structural change.

Chapter 2 - Computational Chemistry

2.1 Introduction

In order to analyze experimental kinetic data in terms of frontier molecular orbital models, it is important to have accurate values for HOMO and LUMO energies, obtainable from ionization potentials according to Koopmans' Theorem[27]. Two forms of the ionization potential may be obtained experimentally:

- The vertical ionization potential (vIP) may be defined as the energy change in a molecule when an electron is ejected *without relaxation of the molecular geometry* (*ie*. where the timescale of ejection << timescale of molecular relaxation).
- The adiabatic ionization potential (IP_{ad}) may be defined as the energy change in a molecule under conditions where the electron is ejected, and relaxation of the molecular geometry is possible either during the ionization, or prior to detection.

The ionization potential may be determined experimentally by two methods: Photoelectron spectroscopy (PES), where electrons are ejected following interaction of a molecule with high frequency radiation, and by electron impact (EI) ionization, where electrons are ejected following collision with an electron of high kinetic energy.[32] Of the two PES is generally considered the more sensitive and accurate method of determining ionization potentials.

In the absence of reliable experimental data, or in cases where experimental data disagree, both vertical and adiabatic ionization potentials may be estimated by high level MO calculations. The ionization potential is the change in energy (typically measured in electron volts, 1 Hartree (a.u.) = 27.21 eV = 627.5 kcal/mol) that occurs upon ionization, that is:

$$IP = E(\text{neutral molecule}) - E(\text{radical cation}) \quad (3)$$

Whether vIP or IP_{ad} is calculated depends on whether the radical cation energy is calculated as a single point energy at the geometry of the neutral molecule, or whether the radical cation geometry is optimized. Calculation of the ionization potentials for all of the olefin and alkyne substrates used by Huisgen[28], and in this study was performed using highly accurate ("chemical accuracy") computational methods.

2.2 Computational Methodologies

All calculations were performed using the *GAUSSIAN 03* program suite[33]. HOMO Energies were initially estimated using Density Functional Theory (DFT), using the Becke 3-parameter functional/Lee-Yang-Parr correlation functional hybrid (B3LYP)**[34-37] with the 6-311G(d,p) basis set. DFT is a semi-empirical method that has about the same computational cost of a Hartree-Fock (HF) calculation, but includes dynamic electron correlation.[38]

Ionization potentials were calculated at the G2(MP2) level of theory. This level of theory is a representative of the composite G*n* levels of theory: these are methods that are designed to provide molecular energies very close to those theoretically obtainable by exact solution of the Schrödinger equation for the molecule. The G2 method involves the

geometry optimization of a molecule at the MP2/6-31G(d) level of theory (Hartree-Fock, with second order Møller-Plesset perturbation corrections to account for some of the electron correlation). A series of single point energies are calculated at various levels of theory, and the G2 Energy is formulated as:

$$E_{G2} = E_{base} + \Delta E^{+} + \Delta E^{2df} + \Delta E^{G2} + \Delta E^{HLC} + ZPE \quad (4)$$

where E_{base} is the single point energy computed at the QCISD(T)/6-311G(d,p) level of theory (a high-level, multi-configurational model), and

$$\Delta E^{+} = E_{MP4/6\text{-}311+G(d,p)} - E_{MP4/6\text{-}311G(d,p)} \quad (5)$$

which corrects for the effect of an additional diffuse function in the basis set.

$$\Delta E^{2df} = E_{MP4/6\text{-}311+G(2df,p)} - E_{MP4/6\text{-}311G(d,p)} \quad (6)$$

which corrects for the effect of additional polarization functions in the basis set - a third set of *f* functions on heavy atoms and a second set of *p* functions on hydrogen atoms.

$$\Delta E^{G2} = E_{MP2/6\text{-}311+G(3df,2p)} - E_{MP2/6\text{-}311+G(d,p)} - E_{MP2/6\text{-}311G(2df,p)} + E_{MP2/6\text{-}311G(d,p)} \quad (7)$$

which makes a correction for additional polarization functions in the basis set and any non-additivity of the corrections in Equations (5) and (6). The energy obtained after these corrections is, in principle, equivalent to the energy calculated at a high level of theory with a very large basis set (QCISD(T)/6-311+G(3df,2p)), but at a much lower computational cost. The final corrections are the vibrational zero point energy (ZPE, calculated at HF/6-31G(d), and corrected by a factor of 0.8929), and the empirical high-level correction ΔE^{HLC}:

$$\Delta E^{HLC} = -0.00019 n_{\alpha} - 0.00481 n_{\beta} \quad (8)$$

where n_α and n_β are the number of valence electrons in the molecule with α and β spin respectively (in the case of radicals, $n_\alpha > n_\beta$). This last correction is empirically derived by comparison of computed G2 energies with a test bank known experimental energies. The G2 model has a mean absolute deviation (MAD) of 1.2 kcal/mol with respect to experimental data, but remains prohibitively expensive for larger systems due to the computation of fourth-order Møller-Plesset (MP4) energies to achieve more complete capture of correlation energies. An alternative method, which uses only second-order (MP2) terms is known as G2(MP2) theory and is significantly cheaper computationally without unduly sacrificing accuracy (MAD = 1.5 kcal/mol). The G2MP2 energy is calculated as follows:

$$E_{G2(MP2)} = E_{base} + \Delta E^{MP2}\ \Delta E^{HLC} + \text{ZPE} \tag{9}$$

where

$$\Delta E^{MP2} = E_{MP2/6\text{-}311+G(3df,2p)} - E_{MP2/6\text{-}311G(d,p)} \tag{10}$$

a single correction for the addition of multiple polarization functions and diffuse functions to the basis set.

2.3 Results and Discussion

G2(MP2) calculations were performed for the alkenes and radical cations associated with alkenes used by Huisgen, and in the current study. Where possible, radical cation energies were calculated both at the neutral molecule geometry (vIP), and at optimized geometries (IP_{ad}, Table 2).

Table 2. G2(MP2) Energies for dipolarophiles utilized in this study and by Huisgen

Dipolarophile	G2MP2 Energies (Hartree)		
	Neutral	Radical Cation	
		Adiabatic	Vertical
Electron-donating groups			
2,3-dihydrofuran	-230.80709	-230.49756	-230.48543
ethyl vinyl ether	-231.99305	-231.67729	-231.65869
n-butyl vinyl ether	-310.44171	-310.12907	-310.10998
1-ethoxy cyclopentene	-348.48405	-348.19781	-348.17666
1,8-diazabicyclo[5.4.0]undec-7-ene	-461.16192	-460.88181	-460.86658
1-pyrrolidino-1-cyclopentene	-405.88208	-405.63267	-405.61671
1-pyrrolidino-1-cyclohexene	-445.11054	-444.86305	-444.84427
N-(1-cyclopenten-1-yl)morpholine	-481.00941	-480.74927	-480.72424
styrene	-309.02104	-308.70570	-308.69664
4-methoxy styrene	-423.37406	-423.08314	-423.07586
4-methyl styrene	-348.25192	-347.94683	-347.93591
4-chloro styrene	-768.16906	-767.85530	-767.84761
Hydrocarbons			
cyclopentene	-194.90471	-194.56878	-194.55865
cyclohexene	-234.13616	-233.80312	-233.79181
bicyclo[2.2.1]hept-2-ene (norbornene)	-272.15773	-271.83124	-271.82061
bicyclo[2.2.1]hepta-2,5-diene (norbornadiene)	-270.93474	-270.62603	-270.60896
bicyclo[2.2.2]oct-2-ene	-310.19018	-309.87711	-309.85791
hept-1-ene	-274.54066	-274.19544	-274.17978
1-methylcyclopentene	-234.13644	-233.81658	-233.80612
isoprene	-194.86017	-194.56279	-194.55557
Electron-withdrawing groups			
methyl vinyl ketone	-230.82157	-230.46264	-230.45891
methyl acrylate	-305.97105	-305.59436	-305.55307
ethyl acrylate	-345.20019	-344.82909	-344.78879
tert-butyl acrylate	-423.66015	-423.30065	-423.28705
acrylonitrile	-170.53019	-170.12677	-170.12154
dimethyl maleate	-533.52041	-533.17094	-533.13912
methyl crotonate	-345.20068	-344.83563	-344.82336
methyl methacrylate	-345.20117		
diethyl fumarate	-611.98528		-611.59299
maleic anhydride	-378.75636	-378.34652	-378.34174
ethyl crotonate	-384.42751	-384.05030	-384.05317
ethyl cinnamate	-575.81026	-575.48982	-575.48179
N-phenylmaleimide	-589.49487	-589.18524	-589.16263
Alkynes			
phenylacetylene	-307.77962	-307.45075	-307.44601
methyl propiolate	-304.73224	-304.34346	-304.32925
ethyl phenylpropiolate	-574.57561	-574.24745	-574.23873
dimethyl acetylenedicarboxylate	-532.27967		-531.85122

Ionization potentials from G2(MP2) and DFT calculations are summarized in Table 3.

Table 3. Computed and experimental ionization potentials for dipolarophiles

Dipolarophile	Ionization Potential (eV) G2(MP2)			B3LYP/6-311G(d,p)	
	IP_{ad}	vIP	Expt	E_{HOMO} (Hartree)	$-E_{HOMO}$[a] (eV)
Electron-donating groups					
2,3-dihydrofuran	8.42	8.75	8.60[b]	-0.214	5.82
ethyl vinyl ether	8.59	9.10	8.98[c]	-0.226	6.15
n-butyl vinyl ether	8.51	9.03		-0.225	6.13
1-ethoxycyclopentene	7.79	8.36		-0.211	5.74
1,8-diazabicyclo[5.4.0]undec-7-ene	7.62	8.04		-0.207	5.63
1-pyrrolidinocyclopentene	6.79	7.22	7.10±0.05[d]	-0.176	4.80
1-pyrrolidinocyclohexene	6.73	7.25	7.15[e]	-0.177	4.81
N-(1-cyclopentenyl)morpholine	7.08	7.76	7.60±0.05[d]	-0.194	5.29
styrene	8.58	8.83	8.48[f]	-0.232	6.30
4-methoxystyrene	7.92	8.11		-0.211	5.74
4-methylstyrene	8.30	8.60	8.20[g]	-0.224	6.10
4-chlorostyrene	8.54	8.75		-0.236	6.42
Hydrocarbons					
cyclopentene	9.14	9.42	9.20[h]	-0.242	6.58
cyclohexene	9.06	9.37	9.09[i]	-0.242	6.60
bicyclo[2.2.1]hept-2-ene	8.88	9.17	9.20[j]	-0.241	6.55
bicyclo[2.2.1]hepta-2,5-diene	8.40	8.86	8.69[k]	-0.227	6.19
bicyclo[2.2.2]oct-2-ene	8.52	9.04	9.05±0.02[l]	-0.235	6.39
hept-1-ene	9.39	9.82	9.27[m]	-0.259	7.03
1-methylcyclopentene	8.70	8.99		-0.231	6.29
isoprene	8.09	8.29	8.85[n]	-0.236	6.43
Electron-withdrawing groups					
methyl vinyl ketone	9.77	9.87	10.11[p]	-0.257	6.98
methyl acrylate	10.25	11.37	10.74[q]	-0.282	7.68
ethyl acrylate	10.10	11.19		-0.280	7.61
tert-butyl acrylate	9.78	10.15		-0.273	7.42
acrylonitrile	10.98	11.12	11.10[r]	-0.299	8.14
dimethyl maleate	9.51	10.38	10.30[s]	-0.274	7.45
methyl crotonate	9.93	10.27		-0.275	7.49
methyl methacrylate			10.06[q]	-0.276	7.50
diethyl fumarate		10.67		-0.286	7.79
maleic anhydride	11.15	11.28	11.07[t]	-0.307	8.36
ethyl crotonate	10.26	10.19	10.11[u]	-0.272	7.41
ethyl cinnamate	8.72	8.94		-0.243	6.62
N-phenylmaleimide	8.43	9.04		-0.247	6.73
Alkynes					
phenylacetylene	8.95	9.08	9.56±0.02[v]	-0.242	6.59
methyl propiolate	10.58	10.97	10.75[r]	-0.290	7.90
ethyl phenylpropiolate	8.93	9.17		-0.247	6.72
dimethyl acetylenedicarboxylate		11.66	10.90[u]	-0.298	8.11

[a]vIP according to Koopmans Theorem. [b-z] See 39-58.

In general terms, there is good agreement between G2(MP2) ionization potentials and experimental ones. The vertical ionization potential was used for structure-reactivity correlations, since the geometry of the dipolarophile is maintained throughout. In any case, there is a strong correlation between the vertical and adiabatic ionization potentials calculated at this level of theory (Figure 7).

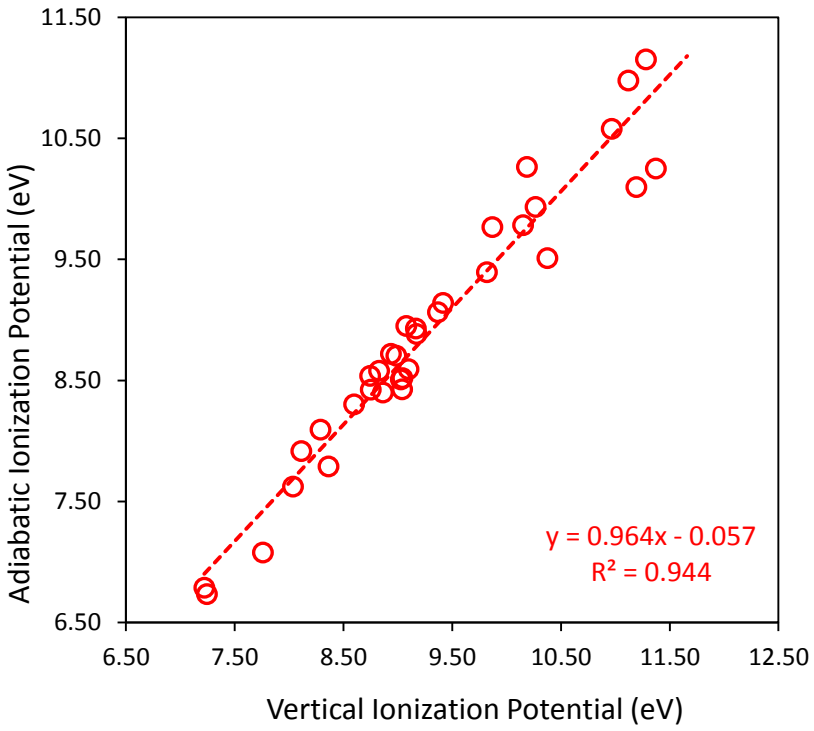

Figure 7. Correlation of vertical and adiabatic ionization potentials for various dipolarophiles calculated at the G2(MP2) level of theory.

DFT calculations have the advantage of generating a set of orbital energies for each dipolarophile (data less readily accessible from composite methods), but it is clear from Table 3 that the computed HOMO energies (equivalent in magnitude to the ionization potential according to Koopmans Theorem) at this level of theory do not show good

agreement with experimental values, with variations of up to 3.7 eV. Nonetheless, a correlation exists between G2(MP2) computed ionization potentials and those calculated via DFT methods (Figure 8). Thus it should be possible in principle to utilize low level calculations to estimate high-level values. In this particular instance, the systems under study are sufficiently small to allow all dipolarophile substrates to be calculated at the higher level of theory.

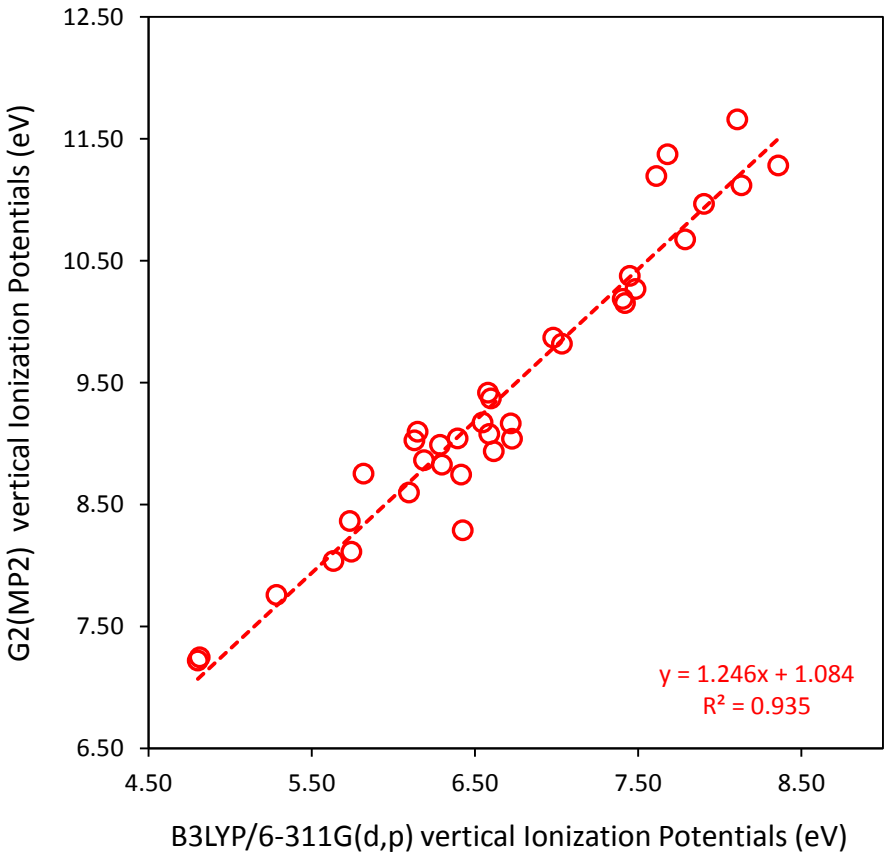

Figure 8. Correlation of vertical ionization potentials for various dipolarophiles calculated at the G2(MP2) and B3LYP/6-311G(d,p) level of theory.

It is important to ensure that the ionization potentials obtained at the G2(MP2) level of theory reproduce the available experimental data. The bulk of the reliable experimental

data have been obtained via photoelectron spectroscopy, which would be expected to correlate to vertical ionization potentials (although there exists a correlation between vertical and adiabatic ionization potentials for these compounds, see Figure 7). Figure 9 shows the correlation between experimental and computed vertical ionization potentials, and a high degree of correlation (R^2 = 0.95) is observed.

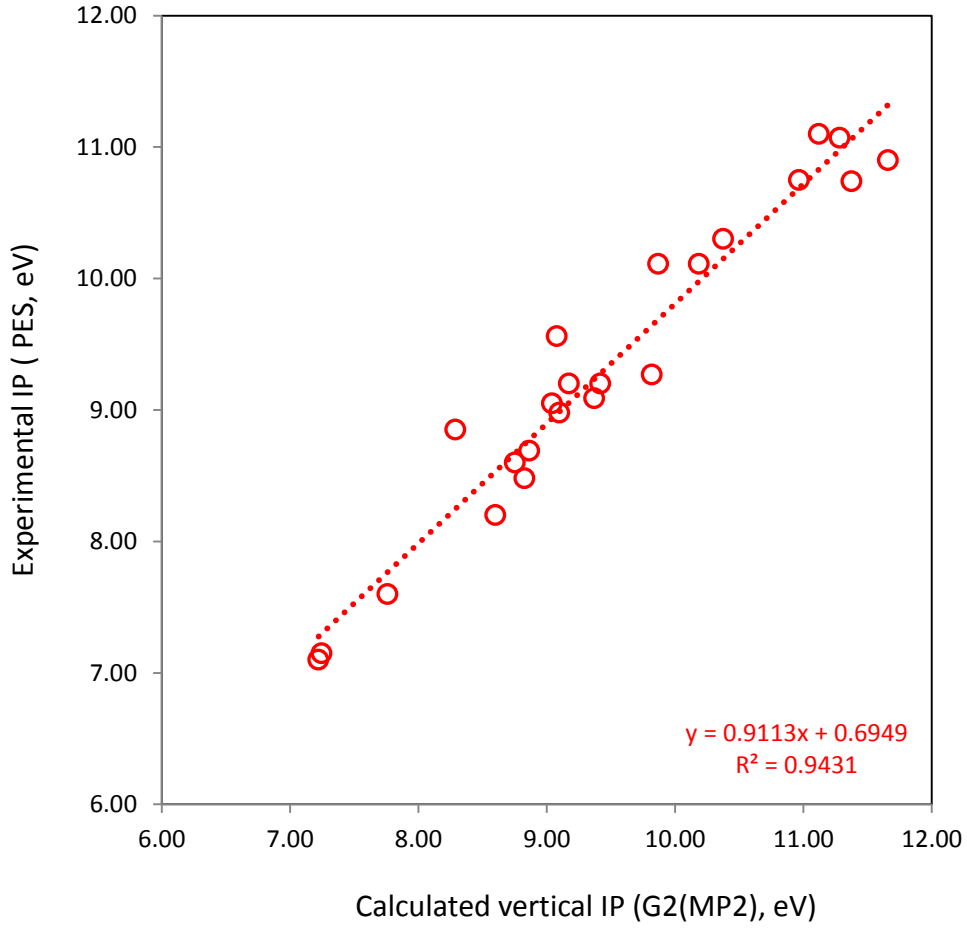

Figure 9. Correlation of vertical ionization potentials and experimental ionization potentials from photoelectron spectroscopy.

It should be noted that the slope of the correlation curve is not 1, and thus the computed ionization potentials have a tendency to be slightly higher than the experimental values.

There are significant outliers; interestingly these correspond to isoprene, phenylacetylene, and 1-heptene, which do not contain particularly complex or polar groups. There is no clear indication of what factors may be responsible for these variations. Nonetheless, it can be concluded that in general terms, the computed ionization potential provides an adequate model that can provide appropriate vertical ionization potentials of species for which no experimental data have been determined.

It is important to note that whilst the kinetic experiments carried out by Huisgen (and in this study) were performed in solvent, ionization potentials were measured and/or calculated in the gas phase, with no consideration to solvent effects. It would be advantageous to look at these effects in the future because in the generation of a radical cation solvent effects may play a major role in stabilizing the charge. Unfortunately, although considerable progress has been made in modeling solvent interactions (using approaches such as polarizable continuum (PCM) models), these have yet to be incorporated into and assessed for composite methods such as G2 and G2(MP2).

Below is a comparison between the calculated vertical ionization potentials to vertical ionization potentials found experimentally by photoelectron spectroscopy. The data shows that our calculations are reasonably close to potentials found in the lab. There are a few outliers and those are isoprene, phenylacetylene, and 1-heptene. This could be due to the presence of a double bond that is capable of reacting differently in the lab than what our calculations could predict.

The calculated vertical ionization potentials provide an opportunity to evaluate the entire Huisgen dataset for reaction of phenyl azide with dipolarophiles (with the exception of methyl

methacrylate, for which calculation of the radical cation proved unsuccessful), rather than the subset considered by Sustmann. The correlation curve for these reactions is shown in Figure 10.

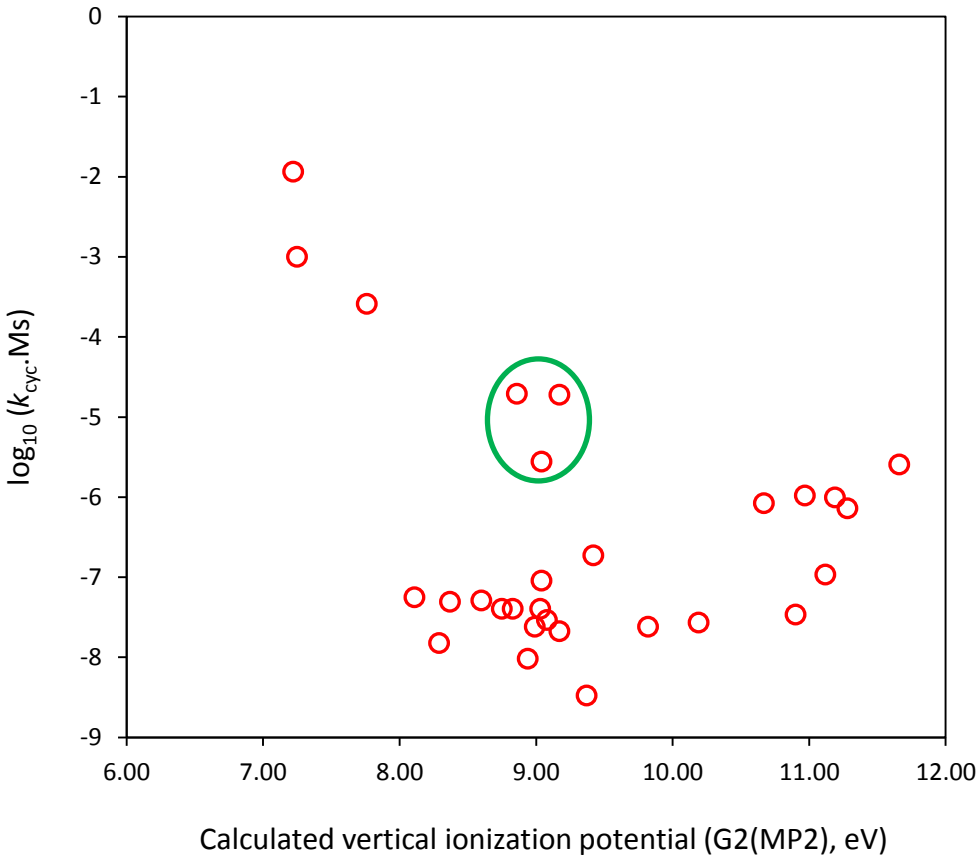

Figure 10. Correlation of calculated (G2(MP2)) vertical ionization potentials and rate coefficients for 1,3-dipolar cycloadditions of phenyl azide (Huisgen). Data circled in green are those for norbornene, norbornadiene and bicyclo[2.2.2]octene.

The expanded data set includes more data points in the region of dipolarophiles that are unsubstituted or have groups without strong electronic effects. It also includes values for the ionization potentials that have been updated since publication of the Sustmann paper (for example, the currently accepted values for styrene and phenylacetylene are

significantly lower than the values used by Sustmann). It could be argued that the curve in Figure 10 is still consistent with Type II dipole behavior as described in Chapter 1, but is not as clear as the previously published data.

In assessing the correlations in Figure 10, it is important to note that the correlation with ionization potential is largely based on enthalpic concerns: that is, the effect of HOMO-LUMO interactions on the enthalpy of activation for the reaction. The ionization potential correlation (and the frontier molecular orbital model upon which it is based), in addition to being based on the assumptions described in Chapter 1, does not explicitly account for entropic effects, nor does it explicitly account for effects that may be encountered in ring systems, such as angle strain.

It is noted that the reaction of cyclopentene with phenyl azide is significantly faster than that of cyclohexene. The angle strain in both cyclohexene and cyclopentene is partially relieved in the transition state, although the initial ring strain in cyclopentene is greater. The relief of ring strain partially offsets the "intrinsic" (derived from the FMO interactions alone) energy cost for cycloaddition of an unfunctionalized alkene to phenyl azide, leading to a decrease in the activation energy, which will be larger for cyclopentene than cyclohexene. Note that the data circled in green in Figure 10, which could be argued to be the data that makes the type II dipole behavior of phenyl azide less clear, are the data for the strained bicyclic systems norbornene, norbornadiene and bicyclo[2.2.1]octene. The lower rate of cyclohexene relative to an unstrained system such as 1-hexene may be ascribed in part to the difference in steric accessibility of a monosusbstituted, as opposed to disubstituted alkene. Clearly no single interaction will provide a universally applicable model to these systems.

Chapter 3 – Kinetics of Cycloaddition of Azidopyridine *N*-Oxides

3.1 Materials & Methods

All materials were purchased from various commercial sources. Dipolarophiles were used after purification through basic alumina. Acetyl chloride, morpholine, and cyclopentanone were distilled prior to use.

NMR spectra were obtained on a 300MHz JEOL Eclipse 300 Multinuclear NMR Spectrometer. IR spectra were obtained on a Perkin-Elmer Spectrum 100 FT-IR Spectrometer.

Kinetic Studies using HPLC Analysis. The following procedure for kinetic studies is typical: 15.7mg of 4-azidopyridine-*N*-oxide was added to 6.4mg of naphthalene (internal standard) in a Reacti-vial,™ and dissolved in a mixture of 1750µL of acetonitrile and 250µL of 2,3-dihydrofuran. Dihydrofuran had previously been filtered through basic alumina to remove any phenolic stabilizers. The solution was stirred vigorously in an oil bath at 35ºC, and 20µL aliquots were taken at 15 minute intervals, diluted with 150µL of methanol, and subjected to HPLC analysis.

High Performance Liquid Chromatography was performed with a Waters 2695 Separations Module attached to a Waters 2996 Photodiode Array Detector (220-450 nm range) with a Dionex Acclaim 120 C-18 5µ (4.6mm x 150mm) column. Injections were

performed in duplicate at 2.5 µL per injection. Solutions were eluted using a water/methanol gradient, using the gradient profile below:

time	0	3	9	13	17	20	22	26	30
%A	11.1	11.1	44.5	72.2	88.9	88.9	44.5	11.1	11.1
%B	88.9	88.9	55.5	27.2	11.1	11.1	55.5	88.9	88.9
Curvature	6	6	6	6	6	6	8	3	6

Where solvent A = 100% Methanol and Solvent B = 10% Methanol/ 90% Milli-Q Water. The gradient curvature is an integer range where 6 is linear, 1 is a step function at the start of the time interval, and 11 is a step function at the end of the time interval.

.

3.1.1 Preparation of 4-Azidopyridine *N*-Oxide (3)

4-Chloropyridine N-oxide. 60mL (800 mmol) of acetyl chloride was added dropwise to 10.02g (71.5 mmol) of 4-nitropyridine *N*-oxide. The mixture was stirred under reflux at 50°C for 45 mins to ensure the production of NO_2 gas had ceased. Excess acetyl chloride was removed by distillation. The mixture was made basic by adding small amounts of saturated Na_2CO_3 solution, and extracted with chloroform (7 x 100mL). The combined extracts were dried over anhydrous Na_2SO_4, and the solvent removed *in vacuo*. The residue was then recrystallized from acetone to yield 4-chloropyridine 1-oxide [5.42g 58% yield], ^{1}H NMR ($CDCl_3$; 400MHz): δ= 8.20 (d, *J*=7.0Hz, 2H); 7.32 (d, *J*= 7.0 Hz, 2H) ppm.

4-Hydrazinopyridine N-oxide. 2.52g (19.4 mmol) of 4-chloropyridine-*N*-oxide and 8.8mL (180 mmol) of hydrazine monohydrate were combined and heated under reflux at 105°C for 30 mins. The reaction mixture was allowed to cool and refrigerated

overnight. The resultant crystals of 4-hydrazinopyridine *N*-oxide [1.46g, 66% crude yield] were collected, and used in the subsequent step without further purification.

4-Azidopyridine N-oxide. A solution of 1.12g of $NaNO_2$ in 12mL of distilled water was added drop wise to a stirred solution of 4-hydrazinopyridine-*N*-oxide in 35mL of 5% HCl in an ice bath. The resultant mixture was allowed to warm to room temperature and stirred for 30 mins, then treated with saturated Na_2CO_3 solution until basic. The mixture was combined with two other batches of similarly treated 4-hydrazinopyridine *N*-oxide, and the combined batches were extracted from chloroform (10 x 50mL), dried over anhydrous Na_2SO_4, and the solvent removed *in vacuo*. The residue was recrystallized from acetone to yield 4-azidopyridine N-oxide [0.159g, 2.5% yield], ^{1}H NMR (D6 DMSO; 300MHz): δ= 8.17 (d, *J*=7.0Hz, 2H); 7.20 (d, *J*= 7.0 Hz, 2H) ppm..

3.1.2 Preparation of 3-Azidopyridine-*N*-oxide (2)

3-Azidopyridine. 4.0g (42.4 mmol) of 3-aminopyridine was dissolved in a solution of 4.8mL of concentrated sulfuric acid and 28mL of distilled water, and the mixture cooled to 0°C. A solution of 2.52g $NaNO_2$ in 20mL of distilled water was added drop wise with stirring, and the solution was allowed to stir for a further 15 mins at 0°C upon completion. A solution of 4.68g (72 mmol) of sodium azide in 16mL of distilled water was added drop wise with vigorous stirring. The solution was stirred a further hour at 0°C, then allowed to warm to room temperature and stirred overnight. The reaction mixture was made basic with saturated Na_2CO_3 solution and and extracted with dichloromethane (3 x 20mL). The combined organic extracts were washed with distilled

water, dried over anhydrous Mg_2SO_4, and stripped of solvent *in vacuo*. The obtained 3-azidopyridine [2.9g, 57% crude yield] was used in the next step without additional purification.

3-Azidopyridine N-oxide. 2.88g of 3-azidopyridine was dissolved in 45mL of glacial acetic acid and 12.2mL of a 30% solution of H_2O_2 was added. The mixture was then heated to 75°C with stirring for 3 hours. At this time a second addition of 4mL of H_2O_2 was added and allowed to heat at 75°C for another 3 hours. The solvent was removed *in vacuo* and then the residue was recrystallized from acetone to provide 3-azidopyridine-*N*-oxide [2.27g, 70% yield], ^{1}H NMR (D_2O; 400MHz): δ= 8.16 (dd, *J*= 1.8, 1.4 Hz, 1H); 8.12 (ddd, *J*= 6.0, 1.4, 1.1 Hz, 1H); 7.60 (dd, *J*= 8.4,6.0 Hz, 1H); 7.53 (ddd, *J*= 8.6, 2.0, 1.1 Hz, 1H) ppm.

3.2 Reactions of Azidopyridine-*N*-oxides with Substrates

3.2.1 Reaction with 2,3-Dihydrofuran

2,3-dihydrofuran (DHF) is a species with an alkene bond adjacent to an electron-donating group. Based on the observed chemistry of phenyl azide, one would expect the cycloaddition to be (a) rapid, and (b) regioselective for a 5-substituted triazoline. Thus, the product of reaction of 2 and 3 with DHF **7** should be the compounds 3- and 4-(1',2',3'-triaza-6'-oxabicyclooct[3.3.0]-2-enyl)pyridine 1-oxide (compounds **8** and **9** respectively, see Scheme 7).

(7)

Scheme 7: Products of 3- and 4-Azidopyridine-*N*-Oxide and DHF

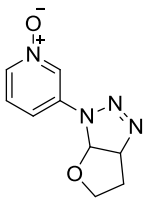

(8)

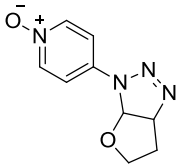

(9)

The cycloaddition reactions generate two new chirality centers. Given that the reaction in question is concerted, a *cis*-relationship between protons on the ring junctions is anticipated, but there is little evidence to expect that the reaction will be enantioselective.

The kinetics of the cycloaddition reaction were determined by monitoring the change in reactant, relative to an internal standard (in this case naphthalene) over time. The data were obtained at relatively low conversions, allowing the reaction to exhibit pseudo first order kinetics (Figure 11). The observed first order rate coefficient, k_{obs} is equivalent to the product of the second order cycloaddition rate coefficient, k_{cyc}, and the concentration of DHF (assumed under pseudo-first-order conditions to be either the starting concentration or average concentration of DHF). In this case, approximately 30 equivalents of DHF was used and the overall conversion is moderate (approximately 50%), so [DHF], to good approximation is unchanged from its initial value.

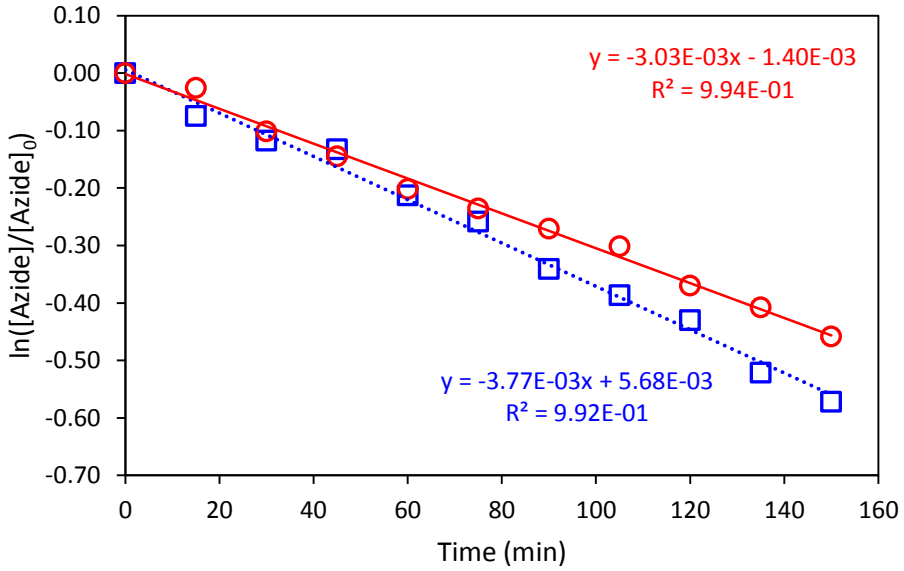

Figure 11. Pseudo-first-order rate curve for cycloaddition of azidopyridine *N*-oxides with DHF at 35°C. Red circles: reaction of 3-azidopyridine *N*-oxide, blue squares: 4-azidopyridine *N*-oxide. The kinetic studies yield second-order rate coefficients, k_{cyc} of 3.05×10^{-5} $M^{-1}s^{-1}$ for the 3-azide 2, and 3.33×10^{-5} $M^{-1}s^{-1}$ for the 4-azide 3 at 35°C.

Attempts were made to isolate and confirm the structures of the cycloadducts of these compounds, and were partially successful. The partially purified ^{1}H NMR spectra (including peak assignments) of the products of **2** and **3** with DHF are shown in Figures 12 and 13 respectively, and are consistent with structures of **8** and **9**. There is no indication of tandem cycloaddition reactions of the type observed previously with methyl acrylate.

3-(1',2',3'-triaza-6'-oxabicyclooct[3.3.0]-2-enyl)pyridine 1-oxide (**7**).

^{1}H NMR ($CDCl_3$, 400 MHz) δ=8.44(dd, *J*= 1.8, 1.8 Hz 1H); 7.93 (ddd, *J*= 6.4, 1.7, 0.9 Hz, 1H); 7.35 (ddd, *J*= 6.2, 1.9, 0.8 Hz, 1H); 7.22 (dd *J*= 8.4, 6.6 Hz, 1H); 5.78 (d, *J*= 6.6 Hz, 1H); 5.21 (t,

J= 7.3, 7.3 Hz, 1H); 3.99 (ddd, *J*= 8.9, 7.8, 1.0 Hz, 1H); 3.18 (ddd, *J*= 11.9, 9.2, 4.9 Hz, 1H); 2.50 (ddd, *J*= 13.2, 5.0, 0.8 Hz, 1H); 2.32 (m, 1H) ppm.

Figure 12 supports the proposed regioselectivity of compound **8** which is evidenced from both the chemical shifts and the vicinal coupling constants. The observed vicinal coupling constant between hydrogens e and f was found to be approximately 6-7Hz and is consistent with the *syn*- relationship that would arise from *cis* regioselectivity because of the magnitude of their interaction with each other. All the remaining hydrogens on the ring are non-equivalent, and their assignments are as follows: Hydrogen d is a ddd with a coupling constants of approximately 8 and 9Hz consistent with a geminal interaction with hydrogen c, strong *vic*- interaction with hydrogen a, and a weak *vic*- interaction with hydrogen b. The remaining signals may be similarly assigned by chemical shift and coupling behavior.

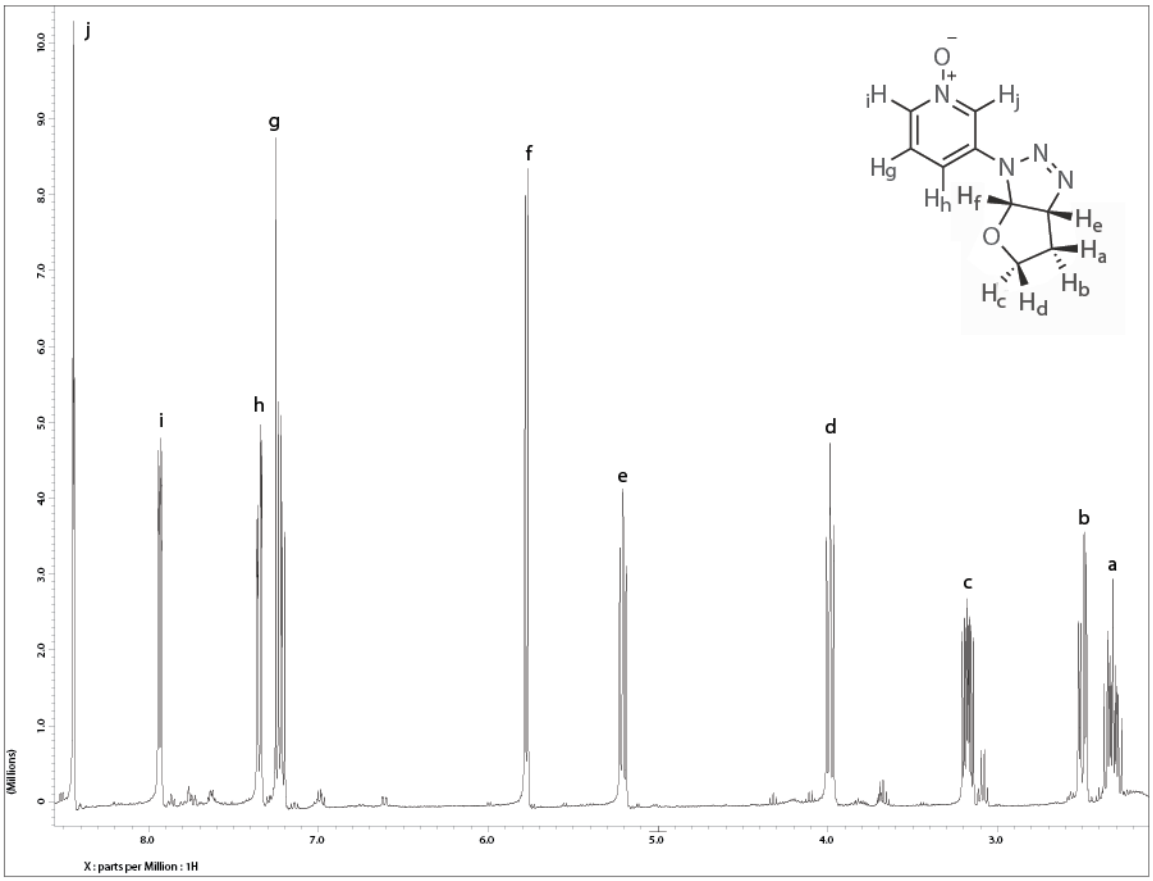

Figure 12. NMR spectra of partially purified 3-(1',2',3'-triaza-6'-oxabicyclooct[3.3.0]-2-enyl)pyridine 1-oxide (8)

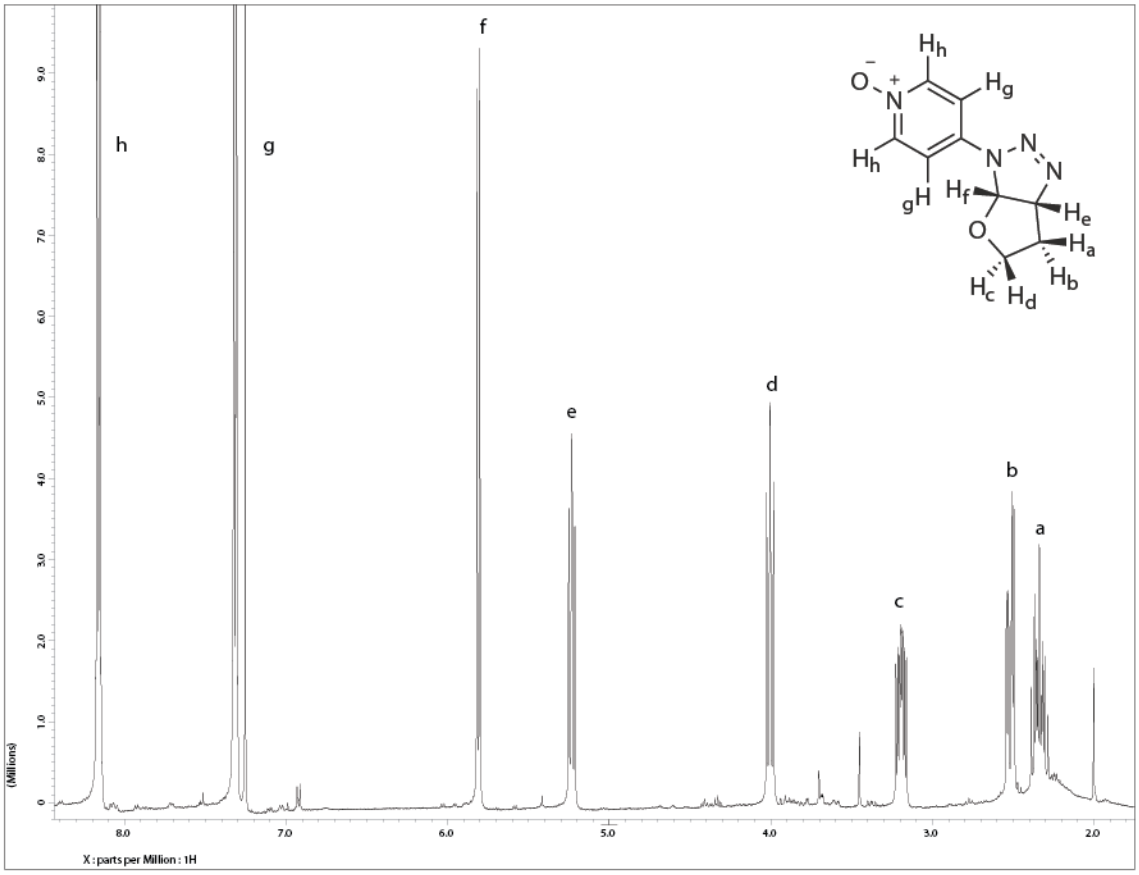

Figure 13. NMR spectra of partially purified 4-(1',2',3'-triaza-6'-oxabicyclooct[3.3.0]-2-enyl)pyridine 1-oxide (9)

3.2.2 Reaction with *tert*-Butyl Acrylate

The reaction of both 4- and 3-azidopyridine-1-oxide with *tert*-butyl acrylate yield dicycloaddition products, and a partially purified ^{1}H NMR spectrum of the diadduct is shown in Figure 14.

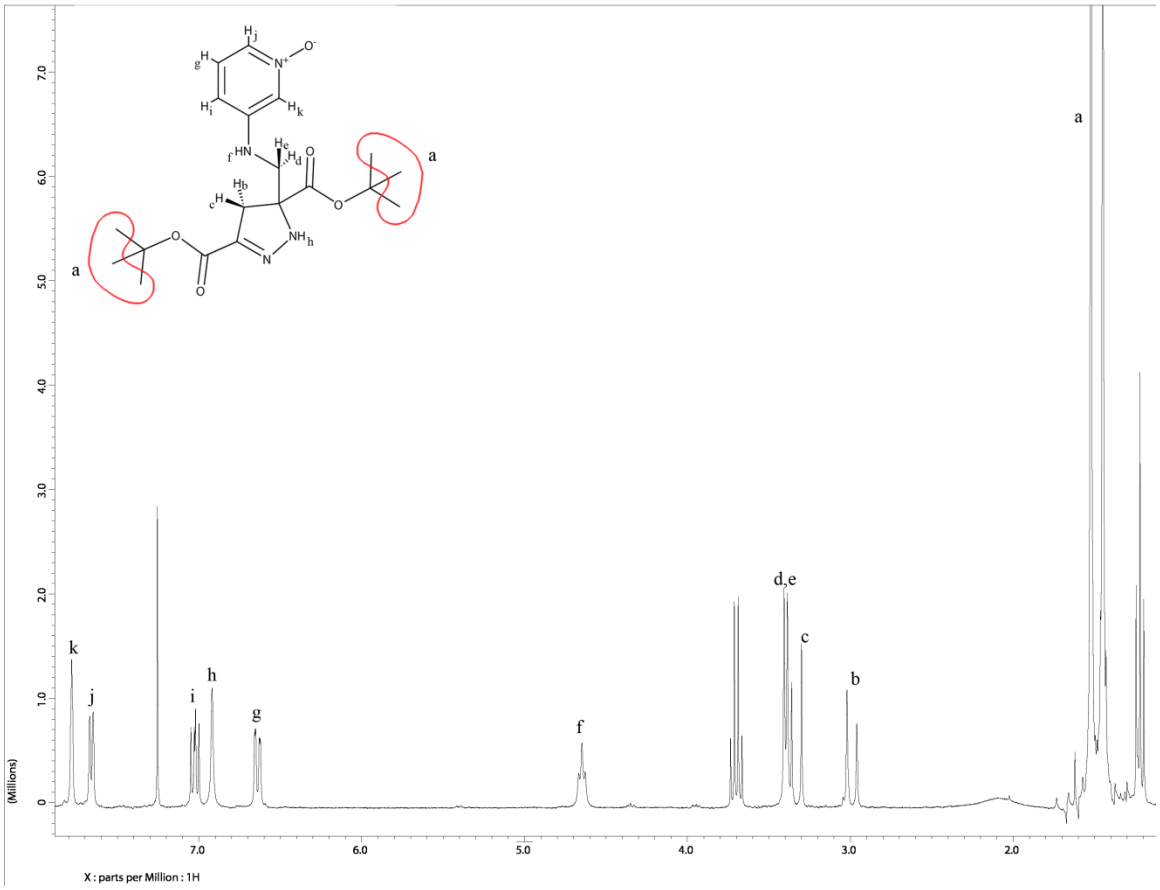

Figure 14 NMR spectra of partially purified N-[(3,5-di t-butoxycarbonyl-4,5-dihydro-1H-pyrazol-5-yl) methyl]-3-aminopyridine-1-oxide. Purification was performed by radial chromatography with an ethanol/chloroform mixture.

N-[(3,5-di *t*-butoxycarbonyl-4,5-dihydro-1H-pyrazol-5-yl) methyl]-3-aminopyridine-1-oxide

^{1}H NMR ($CDCl_3$, 300 MHz) δ= 7.78 (s, 1H); 7.66 (d, *J*= 6.3 Hz, 1H); 7.02 (dd, *J*= 8.4, 1.7 Hz, 1H); 6.92 (s, 1H); 6.64 (dd, *J*= 8.6, 1.7 Hz, 1H); 4.65 (t,*J*= 5.9, 5.9,1H); 3.40 (d, *J*= 6.1 Hz, 2H); 3.33 (d, *J*= 18.2 Hz, 1H); 2.99 (d, *J*= 18.2 Hz, 1H); 1.52 (s, 18H) ppm.

The observed addition reaction exhibited pseudo-first order kinetics (Figure 15). Based on the fact that the diadduct was the major isolable product, it appears that the first cycloaddition is rate-determining.

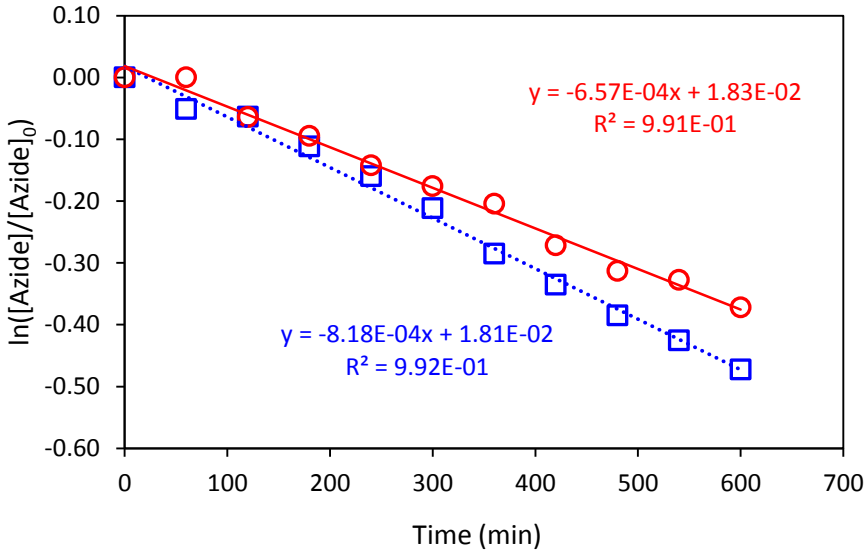

Figure 15. Pseudo-first-order rate curve for cycloaddition of azidopyridine *N*-oxides with tert-butyl acrylate at 35°C. Red circles: reaction of 3-azidopyridine *N*-oxide, blue squares: 4-azidopyridine *N*-oxide. The kinetic studies yield second-order rate coefficients, k_{cyc} of 3.18 x10^{-6} $M^{-1}s^{-1}$ for the 3-azide 2, and 3.87 x10^{-6} $M^{-1}s^{-1}$ for the 4-azide 3 at 35°C.

3.2.3 Reaction with Methyl Propiolate

Reaction of both azides with methyl propiolate exhibits pseudo-first order kinetics (Figure 16) – in these cases the second addition is unfavored as the products of additions are an aromatic 1,2,3-triazoles.(Scheme 8). The rates of reaction are generally comparable to those observed for acrylates, although there appears to be a greater sensitivity to the position of the *N*-oxide moiety on the ring: the 4-azide is some 2-3 times

more reactive than the 3-azide (*cf*. the factors of approximately 1.2-1.3 observed for dihydrofuran and *tert*-butyl acrylate). It would be useful in the future to determine whether this differential reactivity is observed for all reactions leading to triazoles.

Scheme 8: Reactions between azidopyridine-*N*-oxides and methyl propiolate

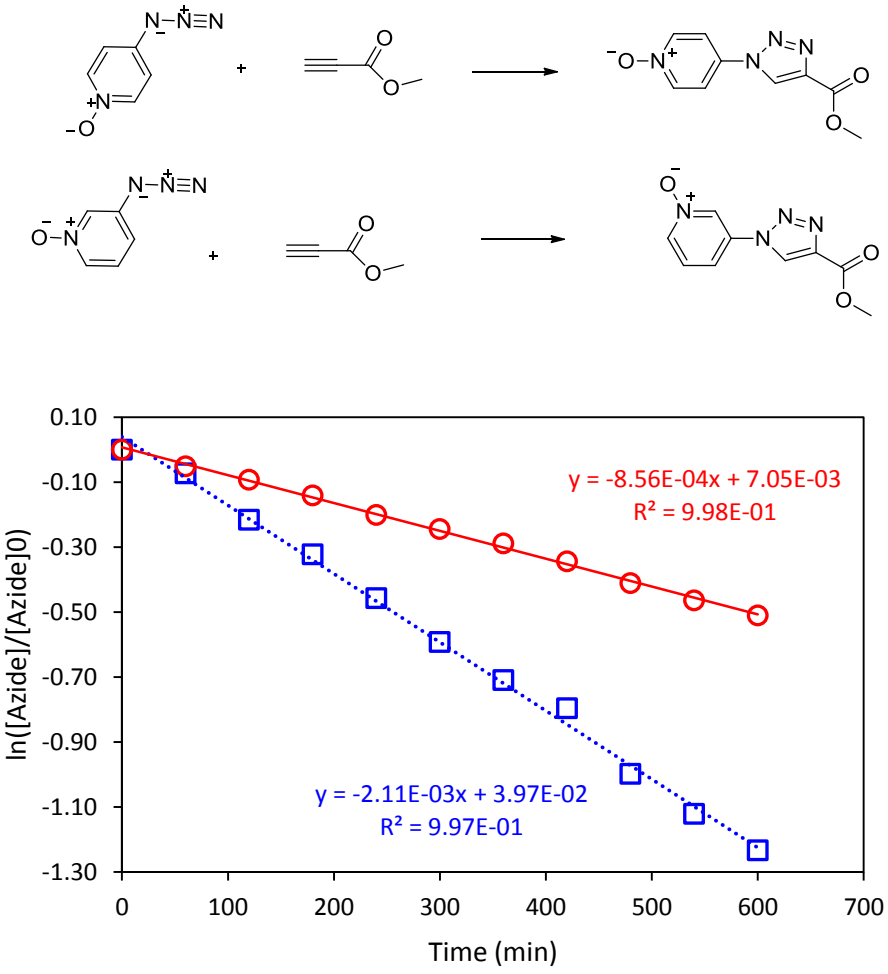

Figure 16. Pseudo-first-order rate curve for cycloaddition of azidopyridine *N*-oxides with methyl propiolate at 35°C. Red circles: reaction of 3-azidopyridine *N*-oxide, blue squares: 4-azidopyridine *N*-oxide. The kinetic studies yield second-order rate coefficients, k_{cyc} of 2.54 x10^{-6} $M^{-1}s^{-1}$ for the 3-azide **2**, and 6.26 x10^{-6} $M^{-1}s^{-1}$ for the 4-azide **3** at 35°C.

3.2.4 Reaction with Ethyl Vinyl Ether

Reaction of 3-azidopyridine 1-oxide with ethyl vinyl ether exhibited pseudo first order kinetics (Figure 17), with a rate coefficient comparable to dihydrofuran.

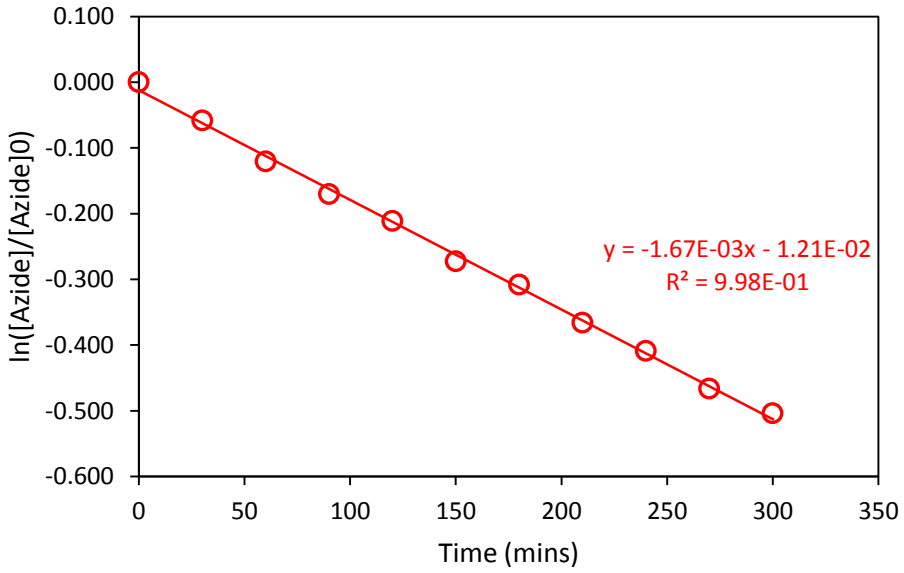

Figure 17. Pseudo-first-order rate curve for cycloaddition of 3-azidopyridine *N*-oxide with ethyl vinyl ether at 35°C. The kinetic study yields second-order rate coefficient, k_{cyc} of 5.33 x10^{-6} $M^{-1}s^{-1}$

3.2.5 Reaction with 1,8-diazabicyclo[5.4.0]undec-7-ene

Reaction of both 3- and 4-azidopyridine-1-oxide with DBU **10** (1,8-diazabicyclo[5.4.0]undec-7-ene) exhibits pseudo first order kinetics for the disappearance of azide (Figure 18).

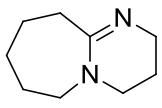

(10)

The structure of the compound formed in these reactions is unknown, and has yet to be isolated. If the reaction does proceed via a simple cycloaddition, then formation of tetrazoline species is indicated (Scheme 10).

Scheme 9: Reaction of 4-azidopyridine *N*-oxide with DBU

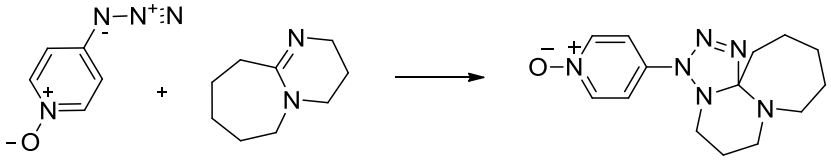

Such a cycloaddition would be significantly different in nature from the others studied in this work (addition to C=N, rather than C=C), and would not necessarily obey a structure-reactivity correlation based on alkene and alkyne addition.

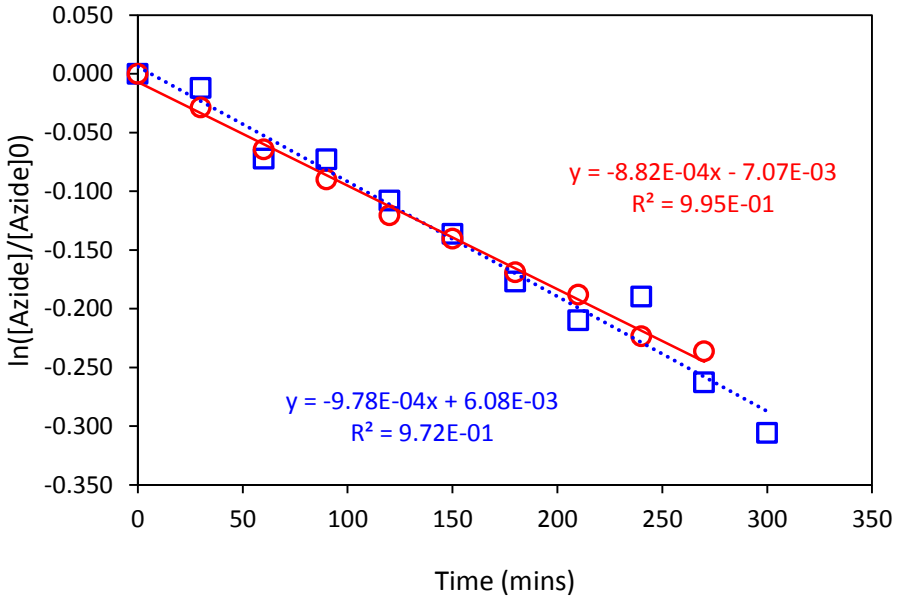

Figure 18. Pseudo-first-order rate curve for cycloaddition of azidopyridine *N*-oxides with DBU at 35°C. Red circles: reaction of 3-azidopyridine *N*-oxide, blue squares: 4-azidopyridine *N*-oxide. The kinetic studies yield second-order rate coefficients, k_{cyc} of 4.40 x10^{-6} $M^{-1}s^{-1}$ for the 3-azide **2**, and 4.88 x10^{-6} $M^{-1}s^{-1}$ for the 4-azide **3** at 35°C.

3.3 Results and Discussion

The second order rate coefficients for reaction of azides with various substrates, derived from the experimentally observed pseudo-first order rate coefficients are tabulated below (Table 4), and a structure-reactivity correlation for these data, as well as previously obtained kinetic data[59], is shown in Figure 19. The correlation is based upon the previously discussed Sustmann model.

Table 4: Derived kinetic data for cycloaddition reactions of azidopyridine-*N*-oxides.

Azide with substrate	k_{cyc}	$\log_{10}(k_{cyc}\cdot Ms)$
	$x10^{-6}$ $M^{-1}s^{-1}$	
3-Azidopyridine-1-oxide		
2,3-Dihydrofuran	30.5 ± 0.8	-4.52 ± 0.03
Ethyl vinyl ether	5.33 ± 0.30	-5.27 ± 0.05
tert-butyl acrylate	3.18 ± 0.10	-5.50 ± 0.03
Methyl propiolate	2.54 ± 0.04	-5.60 ± 0.01
1,8-Diazabicyclo[5.4.0]undec-7-ene	4.40 ± 0.11	-5.36 ± 0.03
4-Azidopyridine-1-oxide		
2,3-Dihydrofuran	33.3 ± 1.0	-4.48 ± 0.03
tert-butyl acrylate	3.87 ± 0.12	-5.41 ± 0.03
Methyl propiolate	6.26 ± 0.12	-5.20 ± 0.02
1,8-Diazabicyclo[5.4.0]undec-7-ene	4.88 ± 0.32	-5.31 ± 0.06

* All errors 95% Confidence Interval on line of best fit

At this stage it is too early to discern whether or not the data exemplifies Type II behavior. The nature of this study was to determine if the presence of the *N*-oxide group played any part in changing the type of interaction in the HOMO-LUMO states (observing Type I or Type III) versus the Type II interaction of phenyl azide. It was originally thought that 3-azidopyridine-N-oxide and 4-azidopyridine-N-oxide would have differences in their rates of reaction due to the capability of the 4-azido compound to

either donate or withdraw electrons through resonance affecting the reactivity. It was observed that 4-azidopyridine-*N*-oxide demonstrated no additional effects and is represented by the data in the graphic. The largest difference observed between the two molecules is approximately 0.4 on a log scale and really isn't much of a big difference. This observed phenomenon means that the structures between the two compounds does not have any effect on the rate of the first cycloaddition, but may play a major role in any second cycloaddition (although this effect is largely invisible due to the non-rate-limiting behavior of the second step. Note that the data points for DBU (on the far left of the correlation curve) do not follow the established (such as it is) correlation.

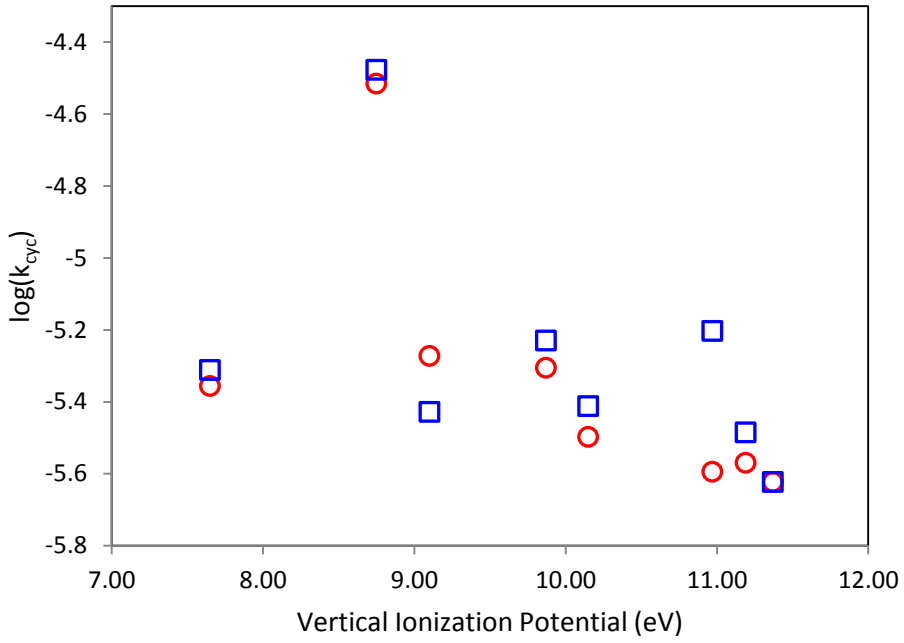

Figure 19. Correlation curve of log(k_{cyc}) and vertical ionization potentials of azidopyridine *N*-oxides. Red circles: 3-azidopyridine *N*-oxide, blue squares: 4-azidopyridine *N*-oxide.

The work to be continued on this project will be to study and determine reaction rates for more dipolarophiles of varying types. This will help define the behavior of the species and further define the type of curve it will show. A study of the reaction rates of phenyl azide and the azidopyridine-N-oxide species with a varying range of dipolarophiles run at the same time at a temperature of 45 ºC and studied via NMR techniques would be advantageous.

Bibliography

1. *Organic Chemistry*, 7th Ed.; McMurry, J.; Thomson : Belmont, CA, **2008**.
2. Bebbington, M.; Szeimies, G.; Mobius, L.; *Coordination Chem. Rev.*, **2009**, 253,1248.
3. Brase, S.; Gil, C.; Knepper, K.; Zimmerman, V.; *Angew. Chem. Int. Ed.*, **2005**, 44,5188.
4. *Azides and Nitrenes - Reactivity and Utility*; Ed: Scriven, E. F. V.; Academic Press: Orlando, FL, **1984**.
5. Pandurangi, R.S.; Kara, S.R.; Kuntz, R.R.; Volkert, W.A.; *Photochemistry and Photobiology*, **1996**, 64, 100.
6. Meijer, E.W.; Nijhuis, S.; Van Vroonhoven, F.C.B.M.; Havinga, E.E.; *NATO ASI series. Series E: Applied Sciences*, **1990**, 192,115.
7. Miller, R.B.; Dugar, S.; Epperson, J.R.; *Heterocycles*, **1987**, 25,217.
8. *1,3-Dipolar Cycloaddition Chemistry*; Ed: Padwa, A.; Wiley-Interscience: New York, **1984**, Vol. I
9. Kolb, H.C.; Finn, M.G.; Sharpless, K.B.; *Angew. Chem. Int. Ed.*, **2001**, 40,2004.
10. Zhang, A.; Slavin, S.; Jones, M.W.; Haddleton, A.J.; Haddleton, D.M.; *Polymer Chemistry*, **2012**, 3,1016.
11. Sivakumar, K.; Xie, F.; Cash, B.M.; Long, S.; Barnhill, H.N.; Wang, Q.; *Org. Lett.*, **2004**, 6,4603.
12. Abramovitch, R.A.; Bachowska, B.; Tomasik, P.; *Polish J. Chem.*, **1984**, 58, 805.
13. Crabtree, K.N.; Hostetler, K.J.; Munsch, T.E.; Neuhaus, P.; Lahti, P.M.; Sander, W.; Poole, J.S.; *J. Org. Chem.*, **2008**, 73, 3441.
14. Poole, J.S.; *J. Mol. Struct.*, **2009**, 894,93.
15. Woodward, R.B.; Hoffmann, R.; *Angew. Chem. Int. Ed.*, **1969**, 8, 781.
16. Xu, L.; Doubleday, C.E.; Houk, K.N.; *J. Am. Chem. Soc.*, **2010**, 132,3029.
17. Lan, Y.; Zou, L.; Cao, Y.; Houk, K.N.; *J. Phys. Chem.*, **2011**, 115, 13906.
18. Houk, K.N.; Sims, J.; C.R.; Luskus, L.J.; *J. Am. Chem. Soc.*, **1973**, 95, 7301.
19. Salem, L.; *J. Am. Chem. Soc.*, **1968**, 90, 543.
20. Salem, L.; *J. Am. Chem. Soc.*, **1968**, 90, 553.
21. Klopman, G.; *J. Am. Chem. Soc.*, **1968**, 90, 223.
22. Herndon, W.C.; *Chem. Rev.*, **1972**, 72, 157.
23. Fukui, K.; *Fortschritte der chemischen Forschun g*, **1970**, 15, 1.
24. Sustmann, R.; *Pure and Applied Chemistry*, **1974**, 40, 569.
25. Hammett, L.P.; *J. Phys. Chem.*, **1936**, 4, 613.
26. Hammett, L.P.; *J. Am. Chem. Soc.*, **1937**, 59, 96.
27. Koopmans, T.; *Physica*, **1933**, 1, 104.
28. Huisgen, R.; Szeimies, G.; Mobius, L.; *Chem. Ber.*, **1967**, 100, 2494.
29. Sustmann, R.; Trill, H.; *Angew. Chem. Int. Ed.*, **1972**, 11, 839.
30. Hostetler, K.J.; M.S. Thesis, Ball State University, **2005**.
31. Yadav, J.S.; Subba Reddy, B.V.; Geetha, V.; *Synlett.*, **2002**, 3, 513.
32. *An Introduction to Molecular Orbitals*; Jean, Y., Volatron, F.; Oxford University Press, **1993**.
33. Gaussian 03, Revision C.02, Frisch, M. J.; Trucks, G. W.; Schlegel, H. B.; Scuseria, G. E.; Robb, M. A.; Cheeseman, J. R.; Montgomery, Jr., J. A.; Vreven, T.; Kudin, K. N.; Burant, J. C.; Millam, J. M.; Iyengar, S. S.; Tomasi, J.; Barone, V.; Mennucci, B.; Cossi, M.; Scalmani, G.; Rega, N.; Petersson, G. A.; Nakatsuji, H.; Hada, M.; Ehara, M.; Toyota, K.; Fukuda, R.; Hasegawa, J.; Ishida, M.; Nakajima, T.; Honda, Y.; Kitao, O.; Nakai, H.; Klene, M.; Li, X.; Knox, J. E.; Hratchian, H. P.; Cross, J. B.; Bakken, V.; Adamo, C.; Jaramillo, J.; Gomperts, R.; Stratmann, R. E.; Yazyev, O.; Austin, A. J.; Cammi, R.; Pomelli, C.; Ochterski, J. W.; Ayala, P. Y.; Morokuma, K.; Voth, G. A.; Salvador, P.; Dannenberg, J. J.; Zakrzewski, V. G.;

Dapprich, S.; Daniels, A. D.; Strain, M. C.; Farkas, O.; Malick, D. K.; Rabuck, A. D.; Raghavachari, K.; Foresman, J. B.; Ortiz, J. V.; Cui, Q.; Baboul, A. G.; Clifford, S.; Cioslowski, J.; Stefanov, B. B.; Liu, G.; Liashenko, A.; Piskorz, P.; Komaromi, I.; Martin, R. L.; Fox, D. J.; Keith, T.; Al-Laham, M. A.; Peng, C. Y.; Nanayakkara, A.; Challacombe, M.; Gill, P. M. W.; Johnson, B.; Chen, W.; Wong, M. W.; Gonzalez, C.; and Pople, J. A.; Gaussian, Inc., Wallingford CT, 2004.

34. Becke,A.D.; *J.Chem.Phys*., **1993**, 98, 5648
35. Lee, C.; Yang, W.; Parr, R.G.; *Phys. Rev*., **1988**, B37, 785
36. Vosko, S.H.; Wilk, L.; Nusair, M.; *Can. J. Phys*., **1980**, 58, 1200
37. Chabalowski, C.F.; Devlin, F.J.; Stephens, P.J.; Frisch, M.J.; *J. Phys. Chem*., **1994**, 98, 11623
38. *Exploring Chemistry With Electronic Structure Methods: A Guide to Using Gaussian*; Foresman, J.B.; Frisch, AE; Gaussian: Pittsburg, PA, **1996**.
39. Batich, C.; Heilbronner, E.; Quinn, C.B.; Wiseman, J.R.; *Helv. Chim. Acta*.,**1976**, 59, 512.
40. Morizur, J.P.; Mercier, J.; Sarraf, M.; *Org. Mass Spectrom.*, **1982**, 17, 327.
41. Domelsmith, L.N.; Houk, K.N.; *Tetrahedron Lett.*, **1972**, 23, 1981.
42. Muller, K.; Previdoli, F.; Desilvestro, H.; *Helv. Chim. Acta*., **1981**, 64, 2497.
43. Kobayashi, T.; *Phys. Lett.*, **1978**, 69, 105.
44. Kobayashi, T.; Yokota, K.; Nagakura, S.; *J. Electron Spectrosc. Relat. Phenom.*, **1973**, 3, 449.
45. Wiberg, K.B.; Ellison, G.B.; Wendoloski, J.J.; Brundle, C.R.; Kuelber, N.A.; *J. Am. Chem. Soc.*, **1976**, 98, 7179.
46. Lambert, J.B.; Zue, L.; Bosch, R.J.; Taba, K.M.; Marko, D.E.; Urano, S.; LeBreton, P.R.; *J. Am. Chem. Soc.*, **1986**, 108, 7575.
47. Wen, A.T.; Hitchcock, A.P.; Westiuk, N.H.; Nguyen, N.; Leigh, W.J.; *Can. J. Chem.*, **1990**, 68, 1976.
48. Houk, K.N.; Rondan, N.G.; Paddon-Ron, M.N.; Jefford, C.W.; Huy, P.T.; Burrow, P.D.; Jordan, K.D.; *J. Am. Chem. Soc.*, **1983**, 105, 5563.
49. Brown, R.S.; Marcinko, R.W.; *J. Am. Chem. Soc*., **1978**, 100, 5721.
50. Ashmore, F.S.;Burgess,A.R.; *J. Chem. Soc. Faraday Trans. 2*, **1978**, *74*, 734.
51. Werstiuk, N.H.; Clark, K.B.; Leigh, W.J.; *Can. J. Chem.*, **1990**, 68, 2078.
52. Kobayashi, T.; *Phys. Lett. A.*, **1978**, 69, 31.
53. Van Dam, H.; Oskam, A; *J. Electron Spectrosc. Relat. Phenom.*, **1978**, 13,273.
54. Bieri, G.; Asbrink, L.; Van Niessan, W.; *J. Electron Spectrosc. Relat. Phenom.*, **1982**, 27, 129.
55. Kobayashi, T.; Yokota, K.; Nagakura, S.; *Bull. Chem. Soc. Jpn.*, **1975**, 48, 412.
56. *Handbook of HeI Photoelectron Spectra of Fundamental Organic Compounds*; Kimura, K.; Katsumata, S.; Achiba, Y.; Yamazaki, T.; Iwata, S.; Japan Scientific Soc. Press, Tokyo, **1981**.
57. Sustmann, R.; Trill, H.; *Tetrahedron Lett.*, **1972**, 42, 4271.
58. Deshmukh, P.; Dutta, T.K.; Hwang, J.L.S; Housecroft, C.E.; Fehlner, T.P.; *J. Am. Chem. Soc.*, **1982**, 104, 1740.
59. Poole, J.S.; private communication.